AD

GRANT NUMBER DAMD17-96-1-6012

TITLE: Computer-Aided Classification of Malignant and Benign Lesions on Mammograms

PRINCIPAL INVESTIGATOR: Berkman Sahiner, M.D.

CONTRACTING ORGANIZATION: University of Michigan
Ann Arbor, Michigan 48103-1274

REPORT DATE: May 1999

TYPE OF REPORT: Annual

PREPARED FOR: Commander
U.S. Army Medical Research and Materiel Command
Fort Detrick, Frederick, Maryland 21702-5012

DISTRIBUTION STATEMENT: Approved for public release;
distribution unlimited

REPORT DOCUMENTATION PAGE

Form Approved
OMB No. 0704-0188

Public reporting burden for this collection of information is estimated to average 1 hour per response, including the time for reviewing instructions, searching existing data sources, gathering and maintaining the data needed, and completing and reviewing the collection of information. Send comments regarding this burden estimate or any other aspect of this collection of information, including suggestions for reducing this burden, to Washington Headquarters Services, Directorate for Information Operations and Reports, 1215 Jefferson Davis Highway, Suite 1204, Arlington, VA 22202-4302, and to the Office of Management and Budget, Paperwork Reduction Project (0704-0188), Washington, DC 20503.

1. AGENCY USE ONLY *(Leave blank)*	2. REPORT DATE	3. REPORT TYPE AND DATES COVERED
	May 1999	Annual (1 May 98 - 30 Apr 99)

4. TITLE AND SUBTITLE
Computer-Aided Classification of Malignant and Benign Lesions on Mammograms

5. FUNDING NUMBERS
DAMD17-96-1-6012

6. AUTHOR(S)
Berkman Sahiner, M.D.

7. PERFORMING ORGANIZATION NAME(S) AND ADDRESS(ES)
University of Michigan
Ann Arbor, Michigan 48103-1274

8. PERFORMING ORGANIZATION REPORT NUMBER

9. SPONSORING/MONITORING AGENCY NAME(S) AND ADDRESS(ES)
Commander
U.S. Army Medical Research and Materiel Command
Fort Detrick, Frederick, Maryland 21702-5012

10. SPONSORING/MONITORING AGENCY REPORT NUMBER

11. SUPPLEMENTARY NOTES

12a. DISTRIBUTION / AVAILABILITY STATEMENT
Approved for public release; distribution unlimited

12b. DISTRIBUTION CODE

13. ABSTRACT *(Maximum 200*

The purpose of this project is to develop computerized classification methods for mammographic abnormalities which will aid radiologists in deciding whether a patient should be biopsied. The regions of interest (ROIs) will be identified by radiologists, and the features to be used in classification will be computer-extracted image features.

In the third year of our project, we developed a segmentation method for delineating boundaries of mammographic masses. New morphological features were extracted from these boundaries. The accuracy of segmentation and the discrimination ability of the extracted morphological features were demonstrated on a data set of 249 biopsy-proven masses. To demonstrate the generalizability of our classification method, a classifier was trained on 301 masses and was tested on 91 independent masses. The classification accuracy on the independent test set (A_Z=0.82) was close to that of an experienced breast radiologist (A_Z=0.88). Morphological features were also extracted for classification of microcalcifications. Their classification accuracy was evaluated on a data set of 145 biopsy proven microcalcifications. The combination of texture and morphological feature spaces for classification of microcalcifications as malignant or benign was also investigated.

14. SUBJECT TERMS
Breast Cancer

15. NUMBER OF PAGES
24

16. PRICE CODE

17. SECURITY CLASSIFICATION OF REPORT	18. SECURITY CLASSIFICATION OF THIS PAGE	19. SECURITY CLASSIFICATION OF ABSTRACT	20. LIMITATION OF ABSTRACT
Unclassified	Unclassified	Unclassified	Unlimited

NSN 7540-01-280-5500

Standard Form 298 (Rev. 2-89)
Prescribed by ANSI Std. Z39-18

FOREWORD

Opinions, interpretations, conclusions and recommendations are those of the author and are not necessarily endorsed by the U.S. Army.

____ Where copyrighted material is quoted, permission has been obtained to use such material.

____ Where material from documents designated for limited distribution is quoted, permission has been obtained to use the material.

✓ Citations of commercial organizations and trade names in this report do not constitute an official Department of Army endorsement or approval of the products or services of these organizations.

____ In conducting research using animals, the investigator(s) adhered to the "Guide for the Care and Use of Laboratory Animals," prepared by the Committee on Care and use of Laboratory Animals of the Institute of Laboratory Resources, national Research Council (NIH Publication No. 86-23, Revised 1985).

✓ For the protection of human subjects, the investigator(s) adhered to policies of applicable Federal Law 45 CFR 46.

____ In conducting research utilizing recombinant DNA technology, the investigator(s) adhered to current guidelines promulgated by the National Institutes of Health.

____ In the conduct of research utilizing recombinant DNA, the investigator(s) adhered to the NIH Guidelines for Research Involving Recombinant DNA Molecules.

____ In the conduct of research involving hazardous organisms, the investigator(s) adhered to the CDC-NIH Guide for Biosafety in Microbiological and Biomedical Laboratories.

June 3, 1999

PI - Signature Date

TABLE OF CONTENTS

INTRODUCTION

Treatment of the breast cancer at an early stage is the most significant means of improving the survival rate of the patients. Mammography is currently the most sensitive method for detecting early breast cancer, and it is also the most practical for screening. However, the positive predictive value of mammographic diagnosis is only about 15%-30%. As the number of patients who undergo mammography increases, it will be increasingly important to improve the positive predictive value of mammography in order to reduce costs and patient discomfort. In this proposal, our goal is to investigate the problem of classifying mammographic lesions as malignant or benign using computer vision, automatic feature extraction, statistical classification, and artificial intelligence techniques. Our efforts are concentrated on the computer-aided classification of two kinds of breast abnormalities, masses and microcalcifications, which are the primary mammographic signs of malignancy. We are investigating computerized extraction of useful features for the differentiation of malignant and benign cases for both abnormalities, and the application of classical statistical classifiers and newly developed paradigms such as neural networks and genetic algorithms for the classification task. Our purposes are to i) improve existing techniques, devise new methods, and identify the preferred approaches for the classification of mammographic lesions, ii) show that computerized classification of mammographic lesions is feasible, and iii) develop a computerized program that can subsequently be shown to improve radiologists' classification of mammographic abnormalities.

BODY

In the third year of the project, we made significant progress in the following areas:

1) Automatic segmentation of breast masses

In the third year of the project, we have developed a segmentation method based on an active contour model and spiculation detection. An active contour is a deformable continuous curve, whose shape is controlled by internal forces (the model, or a-priori knowledge about the object to be segmented) and external forces (the image). In our implementation, the contour is represented by the vertices of a polygon, and a greedy algorithm is used to iteratively minimize the weighted sum of energy components at each vertex. The internal energy components in our active contour model are the continuity and curvature of the contour, and the external energy components are the negative of the smoothed image gradient. The initial set of vertices, the choice of the weights for each energy component, and the smoothing function are important parameters of our segmentation algorithm.

As explained in our previous annual reports, we had already developed a mass segmentation algorithm based on clustering in the first year of the project. We used the result of the clustering-based segmentation as the initial set of vertices for the deformable model. After initial experimentation, we decided to perform the segmentation in two stages. In the first stage, we used an active contour model whose parameters emphasize the smoothness of the mass contour. The resulting first stage segmentation contours are close to the visually perceived object boundaries, but spiculations are not detected. In the second stage, we used a spiculation detection method, which uses the distribution of the angle between θ two vectors for each border pixel b. The first vector is the gradient direction at a pixel in a band around the segmented mass, and the second vector is the direction from this image pixel to the border pixel b. If a spicule

extends from the border pixel b, then θ has a large peak around 90°. By using the statistics of θ, we were able to accurately detect spiculations. On a data set of 249 mammograms (69 spiculated and 180 non-spiculated), we were able to correctly identify 85% of the spiculated masses and 80% of the non-spiculated masses. In the final stage of our algorithm, the spiculations were appended to the already extracted mass shape. Fig. 1 shows the initial mass boundary (result of the clustering algorithm), the output of the active contour model, and final mass boundary for a spiculated and a non-spiculated mass.

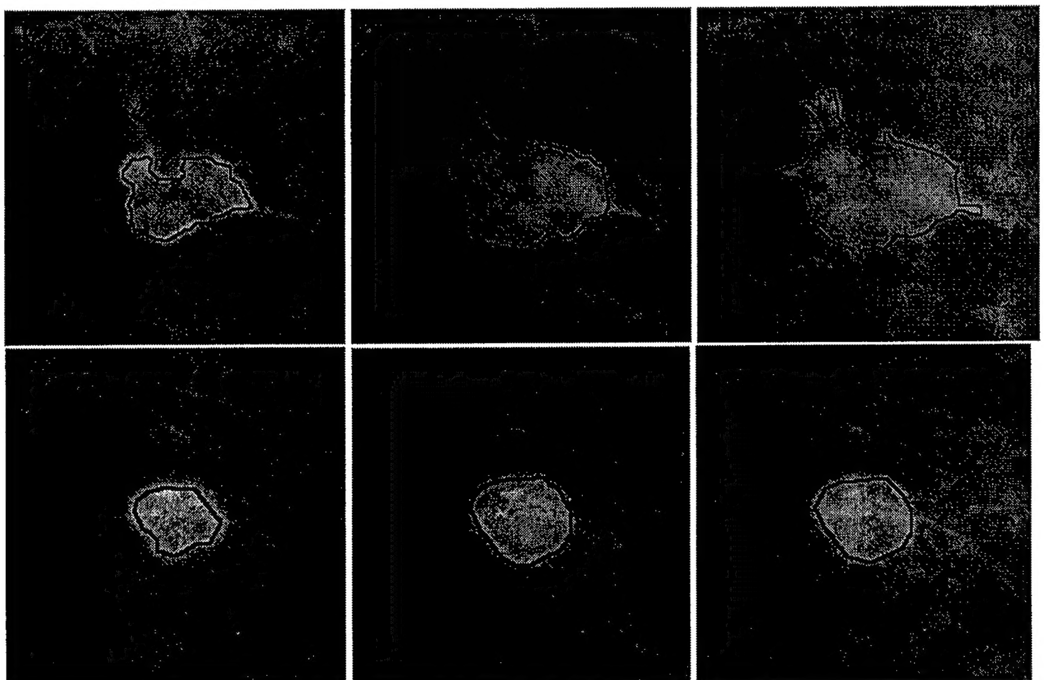

Fig. 1: From left to right, the initial mass boundary, the active contour output, and the final mass boundary. Top row: Spiculated mass, bottom row: Non-spiculated mass

2) Extraction of morphological features for classification of breast masses

Based on the computer segmentation described above, we extracted fourteen morphological features from each mass. The extracted features were a Fourier descriptor feature, two convexity features, the perimeter, area, perimeter-to-area-ratio, circularity, rectangularity, contrast, and five normalized radial length features. Each feature was evaluated for its effectiveness in classifying malignant and benign masses by using the value of the feature as the decision variable in receiver operating characteristic (ROC) analysis, and finding the area A_z under the ROC curve. The Fourier descriptor feature (A_z=0.82) and the convexity features (A_z=0.80 and A_z=0.78) were the most effective features for a data set of 249 masses.

3) Classification of breast masses as malignant or benign using morphological and texture features

We designed classifiers and evaluated their effectiveness with two different data sets using the newly-developed morphological features and the texture features that were developed in the first two years of the project.

The first data set included 249 masses that were previously used for the studying the effectiveness of texture features alone. Using a leave-one-case-out method, and Fischer's linear

discriminant, we obtained a classification accuracy of A_z=0.84 with 5 morphological features selected by stepwise feature selection method. Fifteen features were selected from the combined texture and morphological feature space. The test A_z with these 15 features was 0.93. In comparison, the classification accuracy of a radiologist experienced in mammographic interpretation was A_z=0.91 with the same data set.

The second data set for classifier training included the 249 masses described above, and an additional set of 52 biopsied masses. Feature selection and linear discriminant classifier design were performed using this data set 301 training masses. The designed classifier was then applied to an independent test set of 91 mammograms containing biopsy-proven masses. The test mammograms were digitized using a different digitizer from the training mammograms, and most of them were acquired using a different type of mammographic screen-film system. Therefore, the test conditions were close to a clinical scenario for the application of the classifier. Computerized classification accuracy for the test set was A_z=0.82. A radiologist experienced in mammographic interpretation was asked to rate the test masses for their likelihood of malignancy. The A_z value obtained from the radiologist's ratings was 0.88. This result indicates that the designed classifier may have an acceptable performance when used in a clinical setting. However, the drop in classification accuracy form 0.93 with the initial data set of 249 masses to 0.82 with the independent test set also means that one has to be cautious when generalizing the classification accuracy to a completely independent test set.

4) Extraction of morphological features for classification of microcalcifications

In the third year of the project, we developed morphological feature extraction methods for classification of microcalcifications on mammograms as malignant or benign. For extraction of these features, the locations of individual microcalcifications have to be known. Since detection sensitivity of automated microcalcification programs is not 100%, and since automated methods have a tendency to detect obvious microcalcifications better than subtle microcalcifications, we decided not to use an automatic detection program for determining the location of the microcalcifications. We isolated the detection and classification problems by using manually identified true microcalcification locations. Starting from these locations, and automated region growing technique extracted the signal location as the connected pixels above a gray-level threshold, which was determined as the product of the local root-mean-square noise and an input SNR threshold. After initial experimentation, an SNR threshold of 2.0 was chosen for all cases.

Five features, namely the area, mean density, eccentricity, moment ratio, and area ratio were defined in terms of the first and second moments of the extracted microcalcification signals. To quantify the variation of the visibility of these features, we computed the maximum, average, standard deviation, and the coefficient of variation for each of these features within a cluster. Twenty cluster features were thus defined from the five features of individual microcalcifications. Another feature describing the number of microcalcifications was also added, resulting in a 21-dimensional morphological feature space.

5) Classification of microcalcifications as malignant or benign using morphological and texture features

In the previous two years of the project, we had developed texture feature extraction methods for classification of mammographic microcalcifications as malignant or benign. In the third year of the project, we combined the morphological features with these texture features, and we also investigated the use of two feature selection methods, namely a genetic algorithm (GA) based

feature selection and stepwise linear discriminant analysis (LDA). The classifier was the Fischer's linear discriminant.

Our data set consisted of 145 clusters of microcalcifications from 78 patients. Eighty-two of the microcalcifications were benign and 63 were malignant. The clusters were randomly partitioned into a training set and a test set by an approximately 3:1 ratio. The performance of the trained classifier was evaluated with the test set. In order to reduce the effect of case selection, the random partitioning was performed 50 times, and the results were averaged over the 50 partitions. Table 1 summarizes the classification results (area A_z under the ROC curve) with two different feature selection methods and three feature spaces. Texture features (A_z=0.84) were more effective than morphological features (A_z=0.79). The combined feature space with GA-based feature selection provided the best classification accuracy (A_z=0.90). The improvement in classification accuracy by using the combined feature space was statistically significant in comparison to texture feature space or morphological feature space alone ($p<0.04$).

Table I. Test A_z for classification of microcalcifications as malignant or benign using different feature spaces

	Morphological	Texture	Combined
Genetic Algorithm	0.79±0.07	0.85±0.07	0.90±0.05
Stepwise LDA	0.79±0.07	0.85±0.06	0.87±0.06

6) Database collection

We have continued the collection of mammograms in the third year of this project. We have digitized over 400 new films from over 75 patients where each case contained either a biopsy proven mass or a biopsy proven microcalcification cluster. The expert mammographer in this project, Dr. Mark Helvie has read films of 50 new patients in year three. The new cases will be used as an independent test set in the last year of this project for the evaluation of the classification algorithms.

APPENDIX

Research Accomplishments

- A segmentation method based on an active contour model and a spiculation detection program was developed for segmentation of breast masses on mammograms.
- New morphological features, including a Fourier descriptor feature and two convexity features were developed for classification of masses as malignant or benign.
- The classification accuracy of the morphological features, extracted from the mass boundaries obtained with the new segmentation method, was evaluated using a database of 249 mammograms containing biopsied masses.
- The generalizability of our mass classification method was tested by applying a trained classifier to an independent data set of 91 mammograms containing biopsied masses. Since the test mammograms were digitized using a different digitizer and most of them were acquired using a different type of mammographic screen-film system, the test conditions were close to a clinical scenario for the application of the classifier.

- Morphological features were extracted for the classification of microcalcifications on mammograms as malignant or benign.
- The classification accuracy of the morphological features was evaluated by using the morphological feature space alone and by combining the morhological and texture feature spaces.
- Over 400 new films from over 75 patients were digitized for our database.

Reportable Outcomes

[1] L. Hadjiiski, B. Sahiner, H.-P. Chan, N. Petrick, M.A. Helvie, "Classification of malignant and benign masses based on hybrid ART2LDA approach," submitted to *IEEE Trans. Medical Imaging*, 1998.

[2] H.-P. Chan, B. Sahiner, K.L. Lam, N. Petrick, M.A. Helvie, M.M. Goodsitt, and D.D. Adler, "Computerized analysis of mammographic microcalcifications in morphological and texture feature spaces," *Medical Physics,* 1998, 25:2007-2019.

[3] B. Sahiner, H.-P. Chan, M.A. Helvie, T.E. Wilson, S. Sanjay-Gopal, N. Petrick, "Computerized classification of mammographic masses using morphological features," *84th Scientific Assembly and Annual Meeting of the Radiological Society of North America,* Chicago, IL, Nov. 1998. (Radiology, vol. 209(P), p.353)

[4] L.M. Hadjiiski, B. Sahiner, H.-P. Chan, N. Petrick, M.A. Helvie, M.M. Goodsitt, "Characterization of malignant and benign masses on mammograms based on a hierarchical classifier," *84th Scientific Assembly and Annual Meeting of the Radiological Society of North America*, Chicago, IL, Nov. 1998. (Radiology, vol. 209(P), p.353)

[5] B. Sahiner, H.-P. Chan, N. Petrick, M.A. Helvie, S. Paquerault, L.M. Hadjiiski, "Evaluation of a mammographic mass classifier using an independent data set," submitted to *85th Scientific Assembly and Annual Meeting of the Radiological Society of North America,* Chicago, IL, Nov. 1999.

[6] The P.I. of this project has applied to the Whitaker foundation for a biomedical engineering research grant, and to USAMRMC for an idea grant in 1999. The new grant applications propose to merge the results of the mass classification algorithm developed in the current project with a new computerized classifier that will analyze breast masses on 3-D sonograms.

Computerized analysis of mammographic microcalcifications in morphological and texture feature spaces

Heang-Ping Chan[a)] and Berkman Sahiner
Department of Radiology, University of Michigan, Ann Arbor, Michigan 48109

Kwok Leung Lam
Department of Radiation Oncology, University of Michigan, Ann Arbor, Michigan 48109

Nicholas Petrick, Mark A. Helvie, Mitchell M. Goodsitt, and Dorit D. Adler
Department of Radiology, University of Michigan, Ann Arbor, Michigan 48109

(Received 24 September 1997; accepted for publication 20 July 1998)

We are developing computerized feature extraction and classification methods to analyze malignant and benign microcalcifications on digitized mammograms. Morphological features that described the size, contrast, and shape of microcalcifications and their variations within a cluster were designed to characterize microcalcifications segmented from the mammographic background. Texture features were derived from the spatial gray-level dependence (SGLD) matrices constructed at multiple distances and directions from tissue regions containing microcalcifications. A genetic algorithm (GA) based feature selection technique was used to select the best feature subset from the multi-dimensional feature spaces. The GA-based method was compared to the commonly used feature selection method based on the stepwise linear discriminant analysis (LDA) procedure. Linear discriminant classifiers using the selected features as input predictor variables were formulated for the classification task. The discriminant scores output from the classifiers were analyzed by receiver operating characteristic (ROC) methodology and the classification accuracy was quantified by the area, A_z, under the ROC curve. We analyzed a data set of 145 mammographic microcalcification clusters in this study. It was found that the feature subsets selected by the GA-based method are comparable to or slightly better than those selected by the stepwise LDA method. The texture features ($A_z=0.84$) were more effective than morphological features ($A_z=0.79$) in distinguishing malignant and benign microcalcifications. The highest classification accuracy ($A_z=0.89$) was obtained in the combined texture and morphological feature space. The improvement was statistically significant in comparison to classification in either the morphological ($p=0.002$) or the texture ($p=0.04$) feature space alone. The classifier using the best feature subset from the combined feature space and an appropriate decision threshold could correctly identify 35% of the benign clusters without missing a malignant cluster. When the average discriminant score from all views of the same cluster was used for classification, the A_z value increased to 0.93 and the classifier could identify 50% of the benign clusters at 100% sensitivity for malignancy. Alternatively, if the minimum discriminant score from all views of the same cluster was used, the A_z value would be 0.90 and a specificity of 32% would be obtained at 100% sensitivity. The results of this study indicate the potential of using combined morphological and texture features for computer-aided classification of microcalcifications. [S0094-2405(98)00910-9]

Key words: computer-aided diagnosis, mammography, microcalcifications, genetic algorithm, linear discriminant analysis, ROC analysis

I. INTRODUCTION

Mammography is the most sensitive method for early detection of breast cancers. However, its specificity for differentiating malignant and benign lesions is relatively low. In the United States, the positive predictive value of mammography ranges from about 15% to 30%.[1,2] Various methods are being developed to improve the sensitivity and specificity of breast cancer detection.[3] Computer-aided diagnosis (CAD) is considered to be one of the promising approaches that may improve the efficacy of mammography.[4] Properly designed CAD algorithms can automatically detect suspicious lesions on a mammogram and alert the radiologist to these regions. They can also extract image features from regions of interest (ROIs) and estimate the likelihood of malignancy for a given lesion, thereby providing the radiologist with additional information for making diagnostic decisions.

There are two major approaches to the development of CAD schemes for classification of mammographic abnormalities. One approach uses computer vision techniques to extract image features from the digitized mammograms and classify the lesions based on the computer-extracted features. The computer-extracted features can include morphological features that are commonly used by radiologists for diagno-

sis, as well as texture features that may not be readily perceived by human eyes. The computerized analysis may therefore increase the utilization of mammographic image information and improve the accuracy of differentiating malignant and benign lesions. The other approach uses radiologists' ratings of mammographic features or encodes the radiologists' readings with numerical values. The lesions are then classified based on these radiologist-extracted features. This approach assists radiologists by systematically extracting image features and by optimally merging the features with a statistical classifier to reach a diagnostic decision. Additional risk factors based on patient demographic information and medical or family histories may also be included as input in either approach.

A number of investigators have developed feature extraction and classification methods for characterization of mammographic masses or microcalcifications. Ackerman *et al.*[5] developed 4 measures of malignancy and classified lesions recorded on 120 digitized xeroradiographs by 3 decision methods. Kilday *et al.*[6] used 7 shape descriptors and patient age to classify 39 masses and could correctly classify 69% of the masses. Huo *et al.*[7] analyzed the spiculation of masses using a radial edge-gradient analysis technique and achieved an area, A_z, under the receiver operating characteristic (ROC) curve of 0.88 in a data set of 95 masses. Sahiner *et al.*[8,9] developed a rubber-band straightening image transformation technique to analyze the texture in the region surrounding a mass and obtained an A_z of 0.94 in a data set of 168 masses. Pohlman *et al.*[10] extracted 6 morphological descriptors to classify 47 masses and obtained A_z values ranging from 0.76 to 0.93. Wee *et al.*[11] analyzed 51 microcalcification clusters on specimen radiographs using the average gray level, contrast, and horizontal length of the microcalcifications and obtained 84% correct classification. Fox *et al.*[12] included cluster features in their classifier and obtained 67% correct classification in a data set of 100 clusters from specimen radiographs. Chan *et al.*[13–18] developed morphological and texture features and evaluated various feature classifiers for differentiation of malignant and benign microcalcifications. Shen *et al.*[19] used 3 shape features, compactness, moments, and Fourier descriptors to classify 143 individual microcalcifications with a nearest neighbor classifier and obtained 100% classification accuracy. Wu *et al.*[20] classified 80 pathologic specimens radiographs with a convolution neural network and obtained an A_z of 0.90. Jiang *et al.*[21] trained a neural network classifier to analyze 8 features extracted from microcalcification clusters and obtained an A_z of 0.92 in a data set of 53 patients. Thiele *et al.*[22] extracted texture and fractal features from the tissue region surrounding a microcalcification cluster for classification and achieved a sensitivity of 89% at a specificity of 83% for 54 clusters. Dhawan *et al.*[23] used features derived from first-order and second-order gray-level histogram statistics and obtained an A_z of 0.81 with a neural network classifier for a data set of 191 clusters.

Computerized classification of mammographic lesions using radiologist-extracted features has also been reported by a number of investigators. Ackerman *et al.*[24] estimated the probability of malignancy of mammographic lesions by analyzing 36 radiologist-extracted characteristics with an automatic clustering algorithm and obtained a specificity of 45% at a sensitivity of 100% in a data set of 102 cases. Gale *et al.*[25] analyzed 12 radiologist-extracted features of mammographic lesions with a computer algorithm and obtained a specificity of 88% at a sensitivity of 79% in a data base of 500 patients. Getty *et al.*[26] developed a computer classifier to enhance the differentiation of malignant and benign lesions by a radiologist during interpretation of xeromammograms. Using a similar approach, D'Orsi *et al.*[27] evaluated a computer aid and obtained an improvement of about 0.05 in sensitivity or specificity in mammographic reading. Wu *et al.*[28] trained a neural network to merge 14 radiologist-extracted features for classification of mammographic lesions and obtained an A_z of 0.89. Baker *et al.*[29] trained a neural network based on the lexicon of the Breast Imaging Recording and Data System of the American College of Radiology and found that the neural network could improve the positive predictive value from 35% to 61% in 206 lesions. Lo *et al.*[30] used a similar approach to predict breast cancer invasion and obtained an A_z of 0.91 for 96 lesions. Although the results of these studies varied over a wide range and the performances of the computer algorithms are expected to depend strongly on data set, they indicate the potential of using CAD techniques to improve the diagnostic accuracy of differentiating malignant and benign lesions.

In our early studies, we found that texture features extracted from spatial gray-level dependence (SGLD) matrices at multiple distances were useful for differentiating malignant and benign masses on mammograms. This may be attributed to the texture changes in the breast tissue due to a developing malignancy. The usefulness of SGLD texture measures in differentiating malignant and benign breast tissues was further demonstrated by analysis of mammographic microcalcifications.[17,18,31] In a preliminary study, we developed morphological features to describe the size, shape, and contrast of the individual microcalcifications and their variation within a cluster. We used these features to classify the microcalcifications and obtained moderate results.[13,15] In the present study, we expanded the data set and explored the feasibility of combining texture and morphological features for classification of microcalcifications. The classification accuracy in the combined feature space was compared with those obtained in the texture feature space or in the morphological feature space alone. We also studied the use of a genetic algorithm[32–34] (GA) to select a feature subset from the large-dimension feature spaces, and compared the classification results to those obtained from features selected with stepwise linear discriminant analysis (LDA).[35] Linear discriminant classifiers[36] were designed for the classification tasks. The performance of the classifiers was analyzed with ROC methodology[37] and the classification accuracy was quantified with the area, A_z, under the ROC curve.

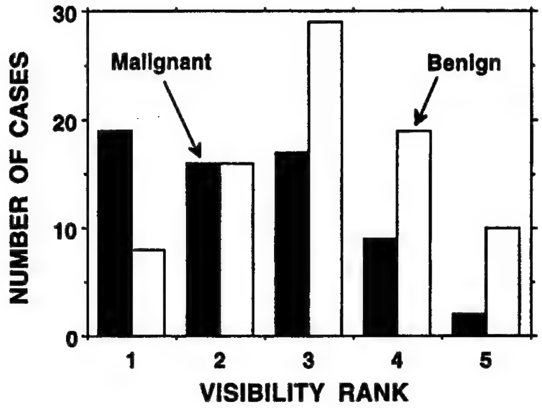

FIG. 1. Distribution of the visibility rankings of the 145 clusters of microcalcifications. Higher ranking corresponds to more subtle clusters.

II. MATERIALS AND METHODS

A. Data set

The data set for this study consisted of 145 clusters of microcalcifications from mammograms of 78 patients. The cases were selected from the patient files in the Department of Radiology at the University of Michigan. The only selection criterion was that it included a biopsy-proven microcalcification cluster. We kept the number of malignant and benign cases reasonably balanced so that 82 benign and 63 malignant clusters were included. All mammograms were acquired with a contact technique using mammography systems accredited by the American College of Radiology (ACR). The dedicated mammographic systems had molybdenum anode and molybdenum filter, 0.3 mm nominal focal spot, reciprocating grid, and Kodak MinR/MinR E screen-film systems with extended processing. A radiologist experienced in mammography ranked the visibility of each microcalcification cluster on a scale of 1 (obvious) to 5 (subtle), relative to the visibility range of microcalcification clusters encountered in clinical practice. The histogram of the visibility ranking of the 145 clusters is shown in Fig. 1. The histogram indicated the mix of subtle and obvious clusters included in the data set.

The selected mammograms were digitized with a laser scanner (Lumisys DIS-1000) at a pixel size of 0.035 mm $\times$0.035 mm and 12-bit gray levels. The digitizer has an optical density (O.D.) range of about 0 to 3.5. The O.D. on the film was digitized linearly to pixel value at a calibration of 0.001 O.D. unit/pixel value in the O.D. range of about 0 to 2.8. The digitizer deviated from a linear response at O.D. higher than 2.8.

B. Morphological feature space

For the extraction of morphological features, the locations of the individual microcalcifications have to be known. We have developed an automated program for detection of individual microcalcifications.[38] However, the detection sensitivity is not 100% and the detected signals include false-positives. Furthermore, automated detection tends to have a higher likelihood of detecting obvious microcalcifications than subtle ones, which may bias the evaluation of the classification capability of the extracted features and the trained classifiers if microcalcifications detected by the automated program are used for classifier development. Since these variables are program dependent, we isolated the detection problem from the classification problem in this study by using manually identified true microcalcifications for the morphological feature analysis. The true microcalcifications were defined as those visible on the film mammograms with a magnifier. Magnification mammograms were used occasionally for verification when they were available, but in most cases only contact mammograms were used. At present, there is no other method that can more reliably identify individual microcalcifications on mammograms. Specimen radiographs can confirm the presence of the microcalcifications but the locations of the individual microcalcifications cannot be correlated with those on the mammograms because of the very different imaging geometry and techniques.

We have developed an automated signal extraction program to determine the size, contrast, signal-to-noise ratio (SNR), and shape of the microcalcifications from a mammogram based on the coordinate of each individual microcalcification. In a local region of 101×101 pixels centered at each signal site, the low frequency structured background is estimated by polynomial curve fitting in the horizontal and vertical directions and then averaging the fitted values obtained in the two directions at each pixel. This background estimation method is used because it can approximate the background more closely than two-dimensional surface fitting or the distance-weighted interpolation method (described below) used for texture feature extraction. The central $l\times l$ pixels that contain the signal are excluded from the curve fitting and noise estimation. The size l is chosen to be a constant of 15 pixels which is larger than the diameters of the microcalcifications of interest yet much smaller than the local region. The background pixel values in this $l\times l$ region are estimated from the fitted and smoothed background surface. The exclusion of the signal region is necessary so that the high contrast pixel values of the microcalcification will not affect the background estimation at the signal site. Other microcalcifications that may locate within the 101×101 pixel region are treated as background pixels because their effect on the estimated background levels at the signal site will be relatively small.

After subtraction of the structured background, the local root-mean-square (rms) noise is calculated. A gray-level threshold is determined as the product of the rms noise and an input SNR threshold. With a region growing technique, the signal region is then extracted as the connected pixels above the threshold around the manually identified signal location. A high threshold will result in extracting only the peak pixels of the microcalcification which may not represent its shape perceived on the mammogram. A low threshold will cause the microcalcification region to grow into the surrounding background pixels. Since there is no objective standard what the actual shape of a microcalcification is on a mammogram, the proper threshold to extract the signals was

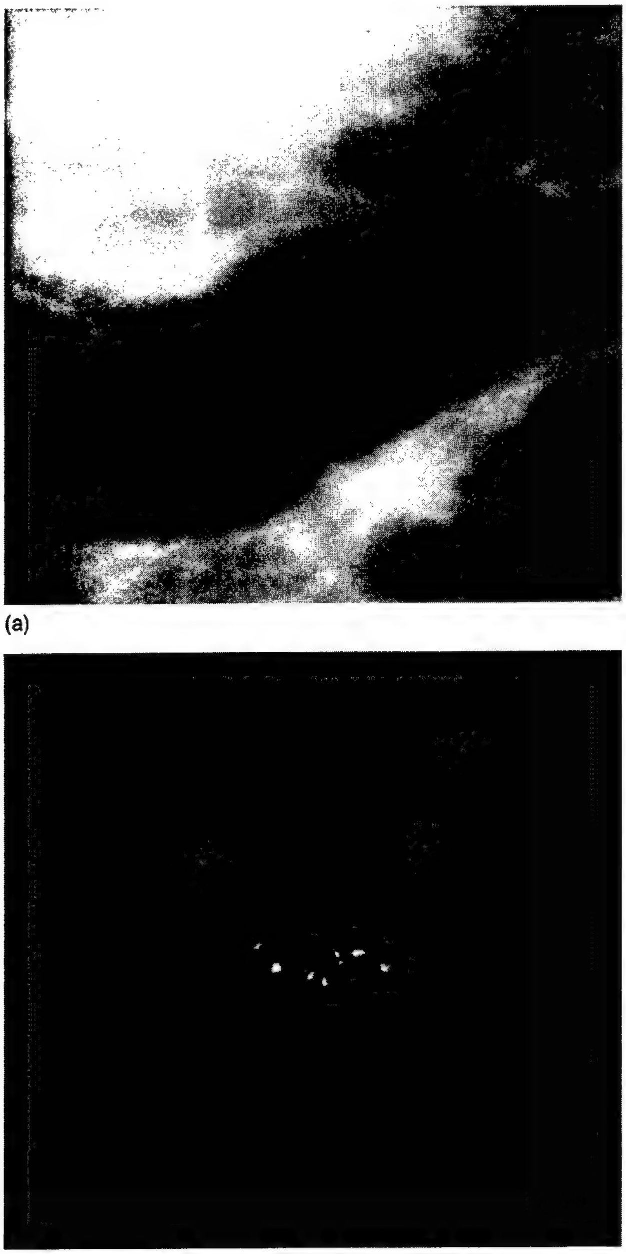

(a)

(b)

FIG. 2. An example of a cluster of malignant microcalcifications in the data set: (a) the cluster with mammographic background, (b) the cluster after segmentation. Morphological features are extracted from the segmented microcalcifications.

determined by visually comparing the microcalcifications in the original image and the thresholded image of the microcalcifications superimposed on a background of constant pixel values. After an experienced radiologist compared a subset of randomly selected microcalcification clusters extracted at different thresholds, an SNR threshold of 2.0 was chosen for all cases. An example of a malignant cluster and the microcalcifications extracted at an SNR threshold of 2.0 is shown in Fig. 2.

The feature descriptors determined from the extracted microcalcifications are listed in Table I. The size of a microcalcification (SA) is estimated as the number of pixels in the signal region. The mean density (MD) is the average of the pixel values above the background level within the signal region. The second moments are calculated as

TABLE I. The 21 morphological features extracted from a microcalcification cluster.

	Average	Standard deviation	Coefficient of variation	Maximum
Area	AVSA	SDSA	CVSA	MXSA
Mean density	AVMD	SDMD	CVMD	MXMD
Eccentricity	AVEC	SDEC	CVEC	MXEC
Moment ratio	AVMR	SDMR	CVMR	MXMR
Axis ratio	AVAR	SDAR	CVAR	MXAR
No. of microcalcifications in cluster	NUMS			

$$M_{xx}=\sum_i g_i(x_i-M_x)^2/M_0, \tag{1}$$

$$M_{yy}=\sum_i g_i(y_i-M_y)^2/M_0, \tag{2}$$

$$M_{xy}=\sum_i g_i(x_i-M_x)(y_i-M_y)/M_0, \tag{3}$$

where g_i is the pixel value above the background, and (x_i,y_i) are the coordinates of the ith pixel. The moments M_0, M_x and M_y are defined as follows:

$$M_0=\sum_i g_i, \tag{4}$$

$$M_x=\sum_i g_ix_i/M_0, \tag{5}$$

$$M_y=\sum_i g_iy_i/M_0. \tag{6}$$

The summations are over all pixels within the signal region. The lengths of the major axis, $2a$, and the minor axis, $2b$, of the effective ellipse that characterizes the second moments are given by

$$2a=\sqrt{2[M_{xx}+M_{yy}+\sqrt{(M_{xx}-M_{yy})^2+4M_{xy}^2}]}, \tag{7}$$

$$2b=\sqrt{2[M_{xx}+M_{yy}-\sqrt{(M_{xx}-M_{yy})^2+4M_{xy}^2}]}. \tag{8}$$

The eccentricity (EC) of the effective ellipse can be derived from the major and minor axes as

$$\epsilon=\frac{\sqrt{a^2-b^2}}{a}. \tag{9}$$

The moment ratio (MR) is defined as the ratio of M_{xx} to M_{yy}, with the larger second moment in the denominator. The axis ratio (AR) is the ratio of the major axis to the minor axis of the effective eclipse.

To quantify the variation of the visibility and shape descriptors in a cluster, the maximum (MX), the average (AV) and the standard deviation (SD) of each feature for the individual microcalcifications in the cluster are calculated. The coefficient of variation (CV), which is the ratio of the SD to AV, is used as a descriptor of the variability of a certain

feature within a cluster. Twenty cluster features are therefore derived from the five features (size, mean density, moment ratio, axis ratio, and eccentricity) of the individual microcalcifications. Another feature describing the number of microcalcifications in a cluster (NUMS) is also added, resulting in a 21-dimensional morphological feature space.

C. Texture feature space

Our texture feature extraction method has been described in detail previously.[31] Briefly, texture features are extracted from a 1024×1024 pixel region of interest (ROI) that contains the cluster of microcalcifications. Most of the clusters in this data set can be contained within the ROI. For the few clusters that are substantially larger than a single ROI, additional ROIs containing the remaining parts of the cluster are extracted and processed in the same way as the other ROIs. The texture feature values extracted from the different ROIs of the same cluster are averaged and the average values are used as the feature values for that cluster.

For a given ROI, background correction is first performed to reduce the low frequency gray-level variation due to the density of the overlapping breast tissue and the x-ray exposure conditions. The gray level at a given pixel of the low frequency background is estimated as the average of the distance-weighted gray levels of four pixels at the intersections of the normals from the given pixel to the four edges of the ROI.[39] The estimated background image was subtracted from the original ROI to obtain a background-corrected image. An example of the background correction procedure is shown in Fig. 3.

As discussed in our previous study,[31] it was found that the texture features derived from the SGLD matrix of the ROI provided useful texture information for classification of microcalcification clusters. The SGLD matrix element, $p_\theta,d(i,j)$, is the joint probability of the occurrence of gray levels i and j for pixel pairs which are separated by a distance d and at a direction θ.[40] The SGLD matrices were constructed from the pixel pairs in a subregion of 512×512 pixels centered approximately at the center of the cluster in the background-corrected ROI so that any potential edge effects caused by background correction will not affect the texture extraction. We analyzed the texture features in four directions: $\theta=0°$, 45°, 90°, and 135° at each pixel pair distance d. The pixel pair distance was varied from 4 to 40 pixels in increments of 4 pixels. Therefore, a total of 40 SGLD matrices were derived from each ROI. The SGLD matrix depends on the bin width (or gray-level interval) used in accumulating the histogram. Based on our previous study, a bin width of four gray levels was chosen for constructing the SGLD matrices. This is equivalent to reducing the gray-level resolution (or bit depth) of the 12-bit image to 10 bits by eliminating the 2 least significant bits.

From each of the SGLD matrices, we derived 13 texture measures including correlation, entropy, energy (angular second moment), inertia, inverse difference moment, sum average, sum entropy, sum variance, difference average, difference entropy, difference variance, information measure of correlation 1, and information measure of correlation 2. The formulation of these texture measures could be found in the literature.[31,40] As found in our previous study,[41] we did not observe a significant dependence of the discriminatory power of the texture features on the direction of the pixel pairs for mammographic textures. However, since the actual distance between the pixel pairs in the diagonal direction was a factor

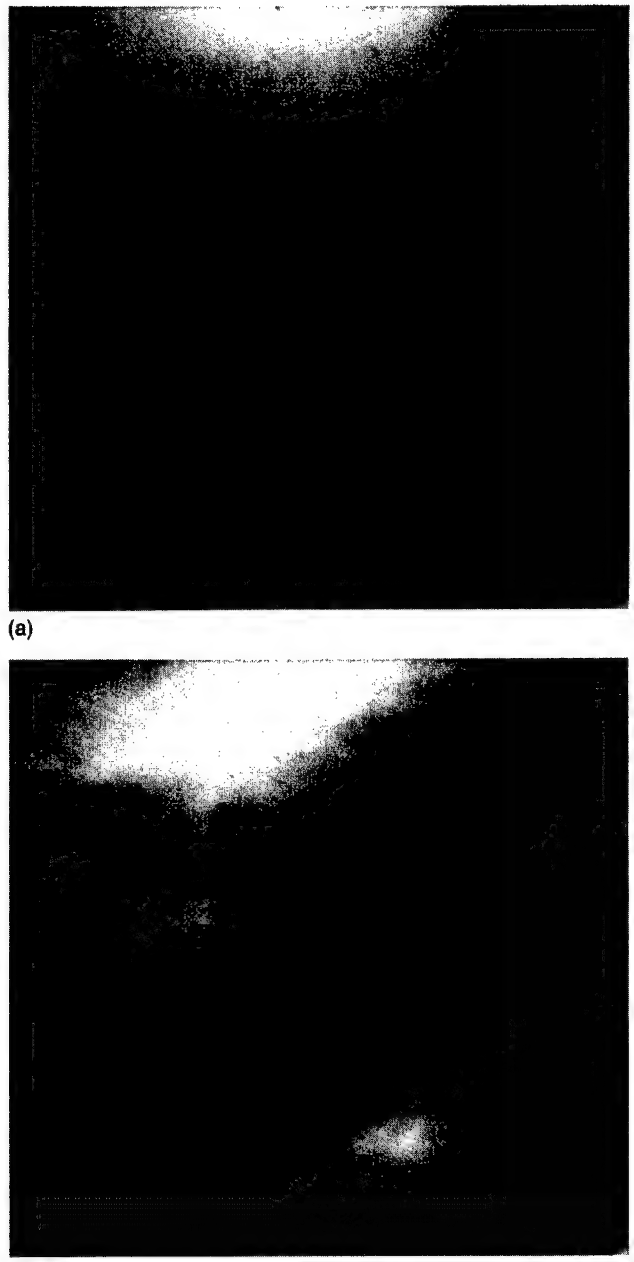

(a)

(b)

FIG. 3. An example of background correction for the ROIs before texture feature extraction. The ROI from the original image is shown in Fig. 2(a). (a) The estimated low frequency background gray level, and (b) the ROI after background correction. The background gray-level variation due to the varying x-ray penetration in the breast tissue is reduced. The contouring in the background image is a display artifact that does not exist in the calculated image file. For display purpose, the background-corrected ROI is contrast-enhanced to improve the visibility of the microcalcifications and the detailed structures.

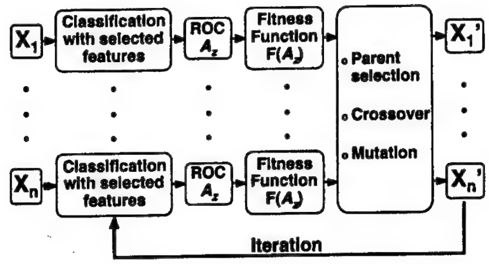

FIG. 4. A schematic diagram of the genetic algorithm designed for feature selection used in this study. $X_1,...,X_n$ represents the set of parent chromosomes and $X_1',...,X_n'$ represents the set of offspring chromosomes.

of $\sqrt{2}$ greater than that in the axial direction, we averaged the feature values in the axial directions (0° and 90°) and in the diagonal directions (45° and 135°) separately for each texture feature derived from the SGLD matrix at a given pixel pair distance. The average texture features at the ten pixel pair distances and two directions formed a 260-dimensional texture feature space.

D. Feature selection

Feature selection is one of the most important steps in classifier design because the presence of ineffective features often degrades the performance of a classifier on test samples. This is partly caused by the "curse of dimensionality" problem that the classifier is inadequately trained in a large-dimension feature space when only a finite number of training samples is available.[42–45] We compared two feature selection methods to extract useful features from the morphological, texture, and the combined feature spaces. One is a genetic algorithm approach, and the other is the commonly used stepwise linear discriminant analysis method.

1. Genetic algorithm for feature selection

The genetic algorithm (GA) methodology was first introduced by Holland in the early 1970s.[32,33] A GA solves an optimization problem based on the principles of natural selection. In natural selection, a population evolves by finding beneficial adaptations to a complex environment. The characteristics of a population are carried onto the next generation by its chromosomes. New characteristics are introduced into a chromosome by crossover and mutation. The probability of survival or reproduction of an individual depends more or less on its fitness to the environment. The population therefore evolves toward better-fit individuals.

The application of GA to feature selection has been described in the literature.[46,47] We have demonstrated previously that a GA could select effective features for classification of masses and normal breast tissue from a very large-dimension feature space.[34] The GA was adapted to the current problem for classification of malignant and benign microcalcifications. A brief outline is given as follows. Each feature in a given feature space is treated as a gene and is encoded by a binary digit (bit) in a chromosome. A "1" represents the presence of the feature and a "0" represents the absence of the feature. The number of genes (bits) on a chromosome is equal to the dimensionality (k) of the feature space, but only the features that are encoded as "1" are actually present in the subset of selected features. A chromosome therefore represents a possible solution to the feature selection problem.

The implementation of GA for feature selection is illustrated in the block diagram shown in Fig. 4. To allow for diversity, a large number, n, of chromosomes, $X_1,..., X_n$, is chosen as the population. The number of chromosomes is kept constant in each generation. At the initiation of the GA, each bit on a chromosome is initialized randomly with a small but equal probability, P_{init}, to be "1." The selected feature subset on a chromosome is used as the input feature variables to a classifier, which was chosen to be the Fischer's linear discriminant in this study.

The available samples in the dataset are randomly partitioned into a training set and a test set. The training set is used to formulate a linear discriminant function with each of the selected feature subsets. The effectiveness of each of the linear discriminants for classification is evaluated with the test set. The classification accuracy is determined as the area, A_z, under the ROC curve. To reduce biases in the classifiers due to case selection, training and testing are performed a large number of times, each with a different random partitioning of the data set. In this study, we chose to partition the dataset 80 times and the 80 test A_z values were averaged and used for determination of the fitness of the chromosome.

The fitness function for the ith chromosome, $F(i)$, is formulated as

$$F(i)=\left[\frac{f(i)-f_{\min}}{f_{\max}-f_{\min}}\right]^2, \quad i=1,...,n, \tag{10}$$

where

$$f(i)=\overline{A_z(i)}-\alpha N(i),$$

$\overline{A_z(i)}$ is the average test A_z for the ith chromosome over the 80 random partitions of the data set, $f_{\min}$ and $f_{\max}$ are the minimum and maximum $f(i)$ among the n chromosomes, $N(i)$ is the number of features in the ith chromosome, and α is a penalty factor, whose magnitude is less than $1/k$, to suppress chromosomes with a large number of selected features. The value of the fitness function $F(i)$ ranges from 0 to 1. The probability of the ith chromosome being selected as a parent, $P_s(i)$, is proportional to its fitness function:

$$P_s(i)=F(i)/\sum_{i=1}^{n} F(i), \quad i=1,...,n. \tag{11}$$

A random sampling based on the probabilities, $P_s(i)$, will allow chromosomes with higher value of fitness to be selected more frequently.

For every pair of selected parent chromosomes, X_i and X_j, a random decision is made to determine if crossover should take place. A uniform random number in (0,1] is generated. If the random number is greater than P_c, the probability of crossover, then no crossover will occur; otherwise, a random crossover site is selected on the pair of chromosomes. Each chromosome is split into two strings at this site and one of the strings will be exchanged with the corre-

sponding string from the other chromosome. Crossover results in two new chromosomes of the same length.

After crossover, another chance of introducing new features is obtained by mutation. Mutation is applied to each gene on every chromosome. For each bit, a uniform random number in (0,1] is generated. If the random number is greater than P_m, the probability of mutation, then no mutation will occur; otherwise, the bit is complemented. The processes of parent selection, crossover, and mutation result in a new generation of n chromosomes, $X_1',\ldots,X_n'$, which will again be evaluated with the 80 training and test set partitions as described above. The chromosomes are allowed to evolve over a preselected number of generations. The best subset of features is chosen to be the chromosome that provides the highest average A_z during the evolution process.

In this study, 500 chromosomes were used in the population. Each chromosome has 281 gene locations. P_{init} was chosen to be 0.01 so that each chromosome started with two to three features on the average. We varied P_c from 0.7 to 0.9, P_m from 0.001 to 0.005, and α from 0 to 0.001. These ranges of parameters were chosen based on our previous experience with other feature selection problems using GA.[34]

2. Stepwise linear discriminant analysis

The stepwise linear discriminant analysis (LDA) is a commonly used method for selection of useful feature variables from a large feature space. Detailed descriptions of this method can be found in the literature.[35] The procedure is briefly outlined below. The stepwise LDA uses a forward selection and backward removal strategy. When a feature is entered into or removed from the model, its effect on the separation of the two classes can be analyzed by several criteria. We use the Wilks' lambda criterion which minimizes the ratio of the within-group sum of squares to the total sum of squares of the two class distributions; the significance of the change in the Wilks' lambda is estimated by F-statistics. In the forward selection step, the features are entered one at a time. The feature variable that causes the most significant change in the Wilks' lambda will be included in the feature set if its F value is greater than the F-to-enter (F_{in}) threshold. In the feature removal step, the features already in the model are eliminated one at a time. The feature variable that causes the least significant change in the Wilks' lambda will be excluded from the feature set if its F value is below the F-to-remove (F_{out}) threshold. The stepwise procedure terminates when the F values for all features not in the model are smaller than the F_{in} threshold and the F values for all features in the model are greater than the F_{out} threshold. The number of selected features will decrease if either the F_{in} threshold or the F_{out} threshold is increased. Therefore, the number of features to be selected can be adjusted by varying the F_{in} and F_{out} values.

E. Classifier

The training and testing procedure described above was used for the purpose of feature selection only. After the best subset of features as determined by either the GA or the stepwise LDA procedure was found, we performed the classification as follows.

The linear discriminant analysis[36] procedure in the SPSS software package[35] was used to classify the malignant and benign microcalcification clusters. We used a cross-validation resampling scheme for training and testing the classifier. The data set of 145 samples was randomly partitioned into a training set and a test set by an approximately 3:1 ratio. The partitioning was constrained so that ROIs from the same patient were always grouped into the same set. The training set was used to determine the coefficients (or weights) of the feature variables in the linear discriminant function. The performance of the trained classifier was evaluated with the test set. In order to reduce the effect of case selection, the random partitioning was performed 50 times. The results were then averaged over the 50 partitions.

The classification accuracy of the LDA was evaluated by ROC methodology. The output discriminant score from the LDA classifier was used as the decision variable in the ROC analysis. The LABROC program,[37] which assumes binormal distributions of the decision variable for the two classes and fits an ROC curve to the classifier output based on maximum-likelihood estimation, was used to estimate the ROC curve of the classifier. The ROC curve represents the relationship between the true-positive fraction (TPF) and the false-positive fraction (FPF) as the decision threshold varies. The area under the ROC curve and the standard deviation of the A_z were provided by the LABROC program for each partition of training and test sets. The average performance of the classifier was estimated as the average of the 50 test A_z values from the 50 random partitions.

To obtain a single distribution of the discriminant scores for the test samples, we performed a leave-one-case-out resampling scheme for training and testing the classifier. In this scheme, one of the 78 cases was left out at a time and the clusters from the other 77 cases were used for formulation of the linear discriminant function. The resulting LDA classifier was used to classify the clusters from the left-out case. The procedure was performed 78 times so that every case was left out once to be the test case. The test discriminant scores from all the clusters were accumulated in a distribution which was then analyzed by the LABROC program. Using the distributions of discriminant scores for the test samples from the leave-one-case-out resampling scheme, the CLABROC program could be used to test the statistical significance of the differences between ROC curves[48] obtained from different conditions. The two-tailed p value for the difference in the areas under the ROC curves was estimated.

III. RESULTS

The variations of best feature set size and classifier performance in terms of A_z with the GA parameters were tabulated in Table II(a)–(c) for the morphological, the texture, and the combined feature spaces, respectively. The number of generations that the chromosomes evolved was fixed at 75

TABLE II. Dependence of feature selection and classifier performance on GA parameters: (a) morphological feature space, (b) texture feature space, and (c) combined feature space. The number of generations that the GA evolved was fixed at 75. The best result for each feature space is identified with an asterisk.

(a)

P_c	P_m	α	No. of features	A_z (Training)	A_z (Test)
0.7	0.001	0	6	0.84	0.79
0.8			3	0.77	0.76
0.9			4	0.80	0.77
0.7	0.003		7	0.82	0.78
0.8			6	0.82	0.79
0.9			6	0.84	0.79
0.7	0.001	0.0005	3	0.77	0.76
0.8			4	0.80	0.77
0.9			3	0.77	0.76
0.7	0.003		6	0.84	0.79*
0.8			6	0.84	0.79
0.9			6	0.82	0.79
0.7	0.001	0.0010	3	0.77	0.76
0.8			4	0.80	0.77
0.9			3	0.77	0.76
0.7	0.003		6	0.84	0.79
0.8			7	0.84	0.79
0.9			4	0.80	0.77

(b)

P_c	P_m	α	No. of features	A_z (Training)	A_z (Test)
0.7	0.001	0	7	0.87	0.82
0.8			8	0.88	0.84
0.9			8	0.88	0.84
0.7	0.003		17	0.91	0.82
0.8			9	0.88	0.79
0.9			10	0.88	0.79
0.7	0.001	0.0005	9	0.88	0.85*
0.8			7	0.86	0.82
0.9			8	0.87	0.84
0.7	0.003		13	0.90	0.81
0.8			10	0.87	0.81
0.9			12	0.88	0.81
0.7	0.001	0.0010	7	0.87	0.83
0.8			9	0.88	0.83
0.9			8	0.88	0.83
0.7	0.003		10	0.88	0.83
0.8			21	0.94	0.82
0.9			12	0.88	0.80

(c)

P_c	P_m	α	No. of features	A_z (Training)	A_z (Test)
0.7	0.001	0	13	0.93	0.88
0.8			12	0.92	0.88
0.9			12	0.92	0.89
0.7	0.003		12	0.91	0.86
0.8			16	0.94	0.88
0.9			17	0.95	0.88
0.7	0.001	0.0003	12	0.92	0.87
0.8			12	0.92	0.86
0.9			12	0.93	0.88
0.7	0.003		13	0.93	0.87
0.8			13	0.93	0.88
0.9			12	0.94	0.89*
0.7	0.005		12	0.89	0.80
0.7	0.001	0.0010	11	0.92	0.87
0.8			10	0.91	0.87
0.9			11	0.91	0.86
0.7	0.003		10	0.91	0.86
0.8			14	0.93	0.87
0.9			13	0.92	0.87
0.7	0.005		11	0.89	0.81
0.8			12	0.88	0.82
0.9			12	0.89	0.81

TABLE III. Dependence of feature selection and classifier performance on F_{out} and F_{in} thresholds using stepwise linear discriminant analysis: (a) morphological feature space, (b) texture feature space, and (c) combined feature space. The best result for each feature space is identified with an asterisk. When the test A_z is comparable, the feature set with fewer number of features is considered to be better.

(a)

F_{out}	F_{in}	No. of features	A_z (Training)	A_z (Test)
2.7	3.8	2	0.76	0.76
1.7	2.8	4	0.79	0.76
1.7	1.8	6	0.83	0.79*
1.0	1.4			
1.0	1.2	7	0.84	0.79
0.8	1.0	9	0.85	0.79
0.6	0.8			
0.4	0.6	10	0.85	0.79
0.2	0.4	12	0.86	0.78
0.1	0.2			

(b)

F_{out}	F_{in}	No. of features	A_z (Training)	A_z (Test)
2.7	3.8	4	0.82	0.80
1.7	2.8			
1.0	1.4	8	0.88	0.83
1.0	1.2	10	0.89	0.82
0.8	1.0	11	0.89	0.83
0.6	0.8	14	0.91	0.85*
0.4	0.6	17	0.92	0.84
0.2	0.4	18	0.92	0.81
0.1	0.2	16	0.90	0.80

(c)

F_{out}	F_{in}	No. of features	A_z (Training)	A_z (Test)
3.0	3.2	6	0.84	0.80
2.9	3.2			
2.8	3.1			
2.0	3.1			
3.0	3.1	10	0.88	0.83
2.9	3.0			
2.7	2.8			
2.0	2.3	11	0.90	0.86
2.0	2.2			
1.9	2.0			
1.7	1.8			
1.3	1.5	14	0.92	0.86
1.0	1.2	19	0.95	0.86
1.0	1.1	23	0.96	0.87*
0.8	1.2	28	0.97	0.86

in these tables. The training and test A_z values were obtained from averaging results of the 50 partitions of the data sets using the selected feature sets.

The results of feature selection using the stepwise LDA procedure with a range of F_{in} and F_{out} thresholds were tabulated in Table III(a)–(c). The thresholds were varied so that the number of selected features varied over a wide range. Often different choices of F_{in} and F_{out} values could result in the same selected feature set as shown in the tables by the number of features in the set. The average A_z values obtained from the 50 partitions of the data set using the selected feature sets were listed. The best feature sets selected in the different feature spaces are shown in Table IV.

TABLE IV. The best feature sets selected by the GA and stepwise LDA methods (indicated by asterisk in Tables II and III) in the three feature spaces. The number of generations for chromosome evolution in the GA algorithm to reach the selected feature sets is listed. The abbreviations for the texture features are: correlation (CORE), energy (ENER), entropy (ENTR), difference average (DFAV), difference entropy (DFEN), difference variance (DFVR), inertia (INER), inverse difference moment (INVD), information measure of correlation 1 (ICO1), information measure of correlation 2 (ICO2), sum average (SMAV), sum entropy (SMEN), sum variance (SMVR). After an abbreviation, the letter "A" indicates diagonal features and the number indicates the pixel distance. The abbreviations for the morphological features can be found in Table I.

GA			Stepwise LDA		
Morphological generation 39	Texture generation 64	Combined generation 169	Morphological	Texture	Combined
CMVD	DFAVA_8	DFAVA_4	AVMD	DFAV_12	CORE_40
CVMR	DFEN_16	DFEN_28	CVMD	DFEN_4	COREA_16
CVSA	DFVRA_24	DFVRA_36	CVMR	DFEN_8	COREA_40
MXMR	DFVR_24	DFVR_12	CVSA	DFENA_12	DFAVA_8
MXSA	DFVR_4	DFVR_20	MXMR	DFENA_24	DFEN_4
SDMD	DFVR_8	ICO1A_20	MXSA	DFVR_24	DFEN_8
	ICO1A_12	ICO1A_32		DFVR_40	DFENA_36
	ICO2A_28	SMEN_16		ICO1_16	DFVR_20
	ICO2_40	SMEN_36		ICO1A_8	ICO1A_28
		AVAR		ICO2_40	ICO2_24
		CVMD		INER_8	ICO2_36
		CVSA		INVD_16	INER_12
		MXEC		INVD_4	INERA_16
		NUMS		INVDA_8	INVDA_36
		SDMD			SMEN_40
					SMENA_4
					AVAR
					CVMD
					CVSA
					MXAR
					MXEC
					NUMS
					SDMD

Table V compares the training and test A_z values from the best feature set in each feature space for the two feature selection methods. The GA parameters that selected the feature set with best classification performance in each feature space after 75 generations (Table II) were used to run the GA again for 500 generations. The A_z values obtained with the best GA selected feature sets after 75 generations are listed together with those obtained after 500 generations. The A_z values obtained with the leave-one-case-out scheme are also shown in Table V. The differences between the corresponding A_z values from the two resampling schemes are within 0.01. The two feature selection methods provided feature sets that had similar test A_z values in the morphological and texture feature spaces. In the combined feature space, there was a slight improvement in the test A_z value obtained with the GA selected features. Although the difference in the A_z

TABLE V. Classification accuracy of linear discriminant classifier in the different feature spaces using feature sets selected by the GA and the stepwise LDA procedure.

	Training A_z			Text A_z		
Feature selection	Morphological	Texture	Combined	Morphological	Texture	Combined
Cross-validation						
GA (75 generations)	0.84±0.04	0.88±0.03	0.94±0.02	0.79±0.07	0.85±0.07	0.89±0.05
GA (500 generations)	0.84±0.04	0.88±0.03	0.96±0.02	0.79±0.07	0.85±0.07	0.90±0.05
Stepwise LDA	0.83±0.04	0.91±0.03	0.96±0.02	0.79±0.07	0.85±0.06	0.87±0.06
Leave-one-case-out						
GA (75 generations)	0.83±0.03	0.88±0.03	0.94±0.02	0.79±0.04	0.84±0.03	0.89±0.03
GA (500 generations)	0.83±0.03	0.88±0.03	0.95±0.02	0.79±0.04	0.84±0.03	0.89±0.03
Stepwise LDA	0.83±0.03	0.91±0.02	0.96±0.02	0.79±0.04	0.85±0.03	0.87±0.03

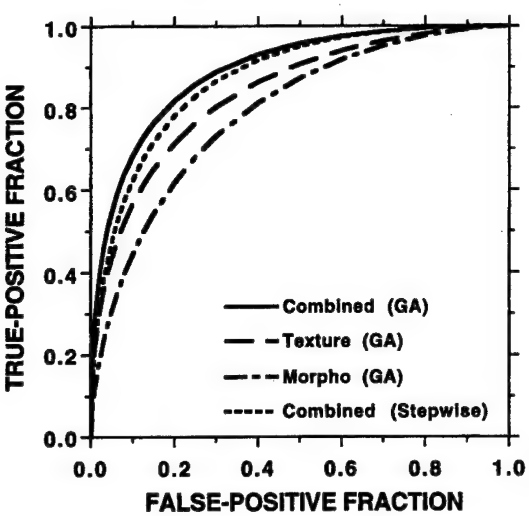

FIG. 5. Comparison of ROC curves of the LDA classifier performance using the best GA selected feature sets in the three feature spaces. In addition, the ROC curve obtained from the best feature set selected by the stepwise LDA procedure in the combined feature space is shown. The classification was performed with a leave-one-case-out resampling scheme.

values from the leave-one-case-out scheme between the two feature selection methods did not achieve statistical significance ($p=0.2$), as estimated by CLABROC, the differences in the paired A_z values from the 50 partitions demonstrated a consistent trend (40 out of 50 partitions) that the A_z from the GA selected features were higher than those obtained by the stepwise LDA. This trend was also observed in our previous study in which mass and normal tissue were classified.[34]

The ROC curves for the test samples using the feature sets selected by the GA were plotted in Fig. 5. The classification accuracy in the combined feature space was significantly higher than those in the morphological ($p=0.002$) or the texture feature space ($p=0.04$) alone. The ROC curve using the feature set selected by the stepwise procedure in the combined feature space was also plotted for comparison. The distribution of the discriminant scores for the test samples using the feature set selected by the GA in the combined feature space is shown in Fig. 6(a). If a decision threshold is chosen at 0.3, 29 of the 82 (35%) benign samples can be correctly classified without missing any malignant clusters.

Some of the 145 samples are different views of the same microcalcification clusters. In clinical practice, the decision regarding a cluster is based on information from all views. If it is desirable to provide the radiologist a single relative malignancy rating for each cluster, two possible strategies may be used to merge the scores from all views: the average score or the minimum score. The latter strategy corresponds to the use of the highest likelihood of malignancy score for the cluster. There were a total of 81 different clusters (44 benign and 37 malignant) from the 78 cases because 3 of the cases contained both a benign and a malignant cluster. The distributions of the average and the minimum discriminant scores of the 81 clusters in the combined feature space were plotted in Fig. 6(b) and Fig. 6(c), respectively. Using the average scores, ROC analysis provided test A_z values of 0.93 ± 0.03

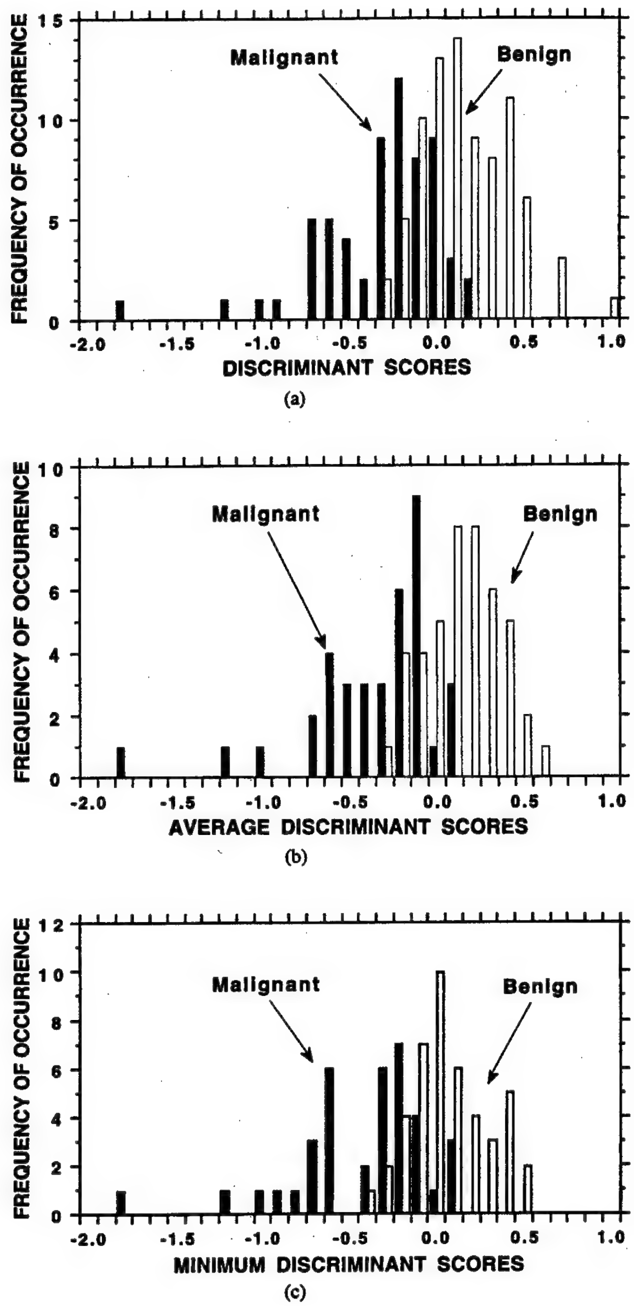

FIG. 6. Distribution of the discriminant scores for the test samples using the best GA selected feature set in the combined texture and morphological feature space. (a) Classification by samples from each film, (b) classification by cluster using the average scores, (c) classification by cluster using the minimum scores.

and 0.89 ± 0.04, respectively, for the GA selected and stepwise LDA selected feature sets. Using the minimum scores, the test A_z values were 0.90 ± 0.03 and 0.85 ± 0.04, respectively. The difference between the A_z values from the two feature selection methods did not achieve statistical significance in either case ($p=0.07$ and $p=0.09$, respectively). If a decision threshold is chosen at an average score of 0.2, 22 of the 44 (50%) benign clusters can be correctly identified with 100% correct classification of the malignant clusters. If a decision threshold is set at a minimum score of 0.2, 14 of the

44 (32%) benign clusters can be identified at 100% sensitivity.

IV. DISCUSSION

The Fischer's linear discriminant is the optimal classifier if the class distributions are multivariate normal with equal covariance matrices.[42] Even if these conditions are not satisfied, as in most classification tasks, the LDA may still be a preferred choice when the number of available training samples is small. Our previous investigation[43,45] of the dependence of classifier performance on design sample size indicated that, in general, the training performance (resubstitution) of a classifier is positively biased whereas the test performance (hold-out) is negatively biased by the sample size. The magnitudes of the biases increase when the dimensionality of the input feature space or the complexity of the classifier increases, or when the design sample size decreases. Therefore, the test performance of a linear classifier is generally better than that of a more complex classifier such as a neural network or a quadratic classifier when the training sample size is small. The training results should not be used for comparison of classifier performance because a classifier can often be overtrained and give a near-perfect classification on training samples while the generalization to any unknown test samples is poor. In this study, we evaluated the effectiveness of using the morphological and the texture features extracted from mammograms for classification of a microcalcification cluster. Although we expanded the data set from our previous study, the current data set was still relatively small. We therefore chose to use a linear discriminant classifier for this classification task. Stepwise feature selection or a GA was used to reduce the dimensionality of the feature space.

In the morphological feature space, the features related to three characteristics, mean density, the moment ratio, and the signal area, were chosen most often. The features related to axis ratio, eccentricity, and the number of microcalcifications in a cluster were chosen only when they were combined with texture features. These results indicate the usefulness of classification in multi-dimensional feature spaces. Some features that are not useful by themselves can become effective features when they are combined with other features. The results also indicate that all six characteristics of the microcalcifications designed for this task have some discriminatory power to distinguish malignant and benign microcalcifications. The morphological features are not as effective as the texture features. This is evident from the smaller A_z values in the morphological feature space. However, when the morphological feature space is combined with the texture feature space, the resulting feature set selected from the combined feature space can significantly improve the classification accuracy, in comparison with those from the individual feature spaces.

The SGLD texture features characterize the shape of the SGLD matrix and generally contain information about the image properties such as homogeneity, contrast, the presence of organized structures, as well as the complexity and gray-level transitions within the image.[40] As an example, the entropy feature measures the uniformity of the SGLD matrix. The entropy value is maximum when all the matrix elements are equal. The entropy value is small when large matrix elements concentrate in a small region of the SGLD matrix while the other matrix elements are relatively small. Therefore, large entropy represents a large but random variation of pixel values in an image without regular structures whereas small entropy represents an image with relatively uniform pixel values if the SGLD matrix peaks along the diagonal and an image with regular texture patterns if it peaks off the diagonal. The ambiguity may be resolved when the sum entropy and difference entropy measures are analyzed. Unlike morphological features, it is difficult, in general, to find the direct relationship between a texture measure and the structures seen on an image,[40] and often a combination of several texture measures extracted at different angles and pixel pair distances are required to describe a texture pattern. It may also be noted that some textures can only be described by second-order statistics and may not be distinguishable by human eyes. The feature selection methods are used to empirically find the combination of features that can most effectively distinguish the malignant and benign lesions.

From Table IV, it can be seen that many of the features in the best feature sets selected by the GA method and the stepwise LDA method are similar. In the morphological feature space, five of the six selected features are the same in the two feature sets. In the combined feature space, six morphological features (out of six and seven morphological features in the two sets, respectively) are the same. For the texture features, there are more variations in the features selected by the two methods. However, the differences are mainly in the pixel distances and the directions of the features, while the major types of the texture features are similar. For example, four types of texture features, energy, entropy, sum average, and sum variance were not selected in either the texture or the combined feature space by both methods. Another four types of texture features, difference average, difference entropy, difference variance, and information measure of correlation 1 were chosen in each case, and information measure of correlation 2 was chosen in three of the four cases. Inertia and inverse difference moment were selected by the stepwise LDA method in both the texture and the combined feature spaces. Sum entropy was selected by both methods in the combined feature space. These results indicate that some features are more effective than the others for distinguishing benign and malignant microcalcifications. The pixel distance and the direction of the texture features may be considered to be higher order effects that have less influence on the discriminatory ability of a given type of texture measure. The smaller differences in their discriminatory ability would subject them to greater variability of being chosen in the feature selection processes. It may also be noted that many of the features are highly correlated. The correlated features can be interchanged in a classifier model without a strong effect on its performance.

The GA solves an optimization problem based on a search guided by the fitness function. Ideally, the values for the P_m,

P_c, and α parameters chosen in the GA only affect the convergence rate but will eventually evolve to the same global maximum. However, when the dimensionality of the feature space is very large and the design samples are sparse, the GA often reaches local maxima corresponding to different feature sets, as can be seen in Table II. Similarly, the stepwise feature selection may reach a different local maximum and choose a feature set different from those chosen by the GA. The different feature sets may provide different or similar performance. The latter is often a result of the correlation among the features, as described above.

For the linear discriminant classifier, the stepwise LDA procedure can select near-optimal features for the classification task. We have shown that the GA could select a feature set comparable to or slightly better than that selected by the stepwise LDA. The number of generations that the GA had to evolve to reach the best selection increased with the dimensionality of the feature space as expected. However, even in a 281-dimensional feature space, it only took 169 generations to find a better feature set than that selected by stepwise LDA. Further search up to 500 generations did not find other feature combinations with better performance. Although the difference in A_z did not achieve statistical significance, probably due to the large standard deviation in A_z when the number of case samples in the ROC analysis was small, the improvements in A_z in this and our previous studies[34] indicate that the GA is a useful feature selection method for classifier design. One of the advantages of GA-based feature selection is that it can search for near-optimal feature sets for any types of linear or nonlinear classifiers, whereas the stepwise LDA procedure is more tailored to linear discriminant classifiers. Furthermore, the fitness function in the GA can be designed such that features with specific characteristics are favored. One of the applications in this direction is to select features to design a classifier with high sensitivity and high specificity for classification of malignant and benign lesions.[49,50] Although the GA requires much longer computation time than the stepwise LDA to search for the best feature set, the flexibility of the GA makes it an increasingly popular alternative for solving machine learning and optimization problems. Since feature selection is performed only during training of a classifier, the speed of a trained classifier for processing test cases is not affected by the choice of the feature selection method. Therefore, the longer computation time of GA is not a problem in practice if the GA can provide a better feature set for a given classification task.

V. CONCLUSIONS

In this study, we evaluated the effectiveness of morphological and texture features extracted from mammograms for classification of malignant and benign microcalcification clusters. We also compared a GA-based feature selection method and a stepwise feature selection procedure based on linear discriminant analysis. It was found that the best feature set was selected from the combined morphological and texture feature space by the GA-based method. A linear discriminant classifier using the best feature set and a properly chosen decision threshold could correctly identify 35% of the benign clusters without missing any malignant clusters. If the average discriminant score from all views of the same cluster was used for classification, the accuracy improved to 50% specificity at 100% sensitivity. Alternatively, if the minimum discriminant score from all views of the same cluster was used, the accuracy would be 32% specificity at 100% sensitivity. This information may be used to reduce unnecessary biopsies, thereby improving the positive predictive value of mammography. Although these results were obtained with a relatively small data set, they demonstrate the potential of using CAD techniques to analyze mammograms and to assist radiologists in making diagnostic decisions. Further studies will be conducted to evaluate the generalizability of our approach in large data sets.

ACKNOWLEDGMENTS

This work is supported by USPHS Grant No. CA 48129 and by U.S. Army Medical Research and Materiel Command Grant No. DAMD 17-96-1-6254. Berkman Sahiner is also supported by a Career Development Award by the U.S. Army Medical Research and Materiel Command (DAMD 17-96-1-6012). Nicholas Petrick is also supported by a grant from The Whitaker Foundation. The content of this publication does not necessarily reflect the position of the government and no official endorsement of any equipment and product of any companies mentioned in the publication should be inferred. The authors are grateful to Charles E. Metz, Ph.D. for use of the LABROC and CLABROC programs.

[a]Electronic mail: chanhp@umich.edu

[1]D. D. Adler and M. A. Helvie, "Mammographic biopsy recommendations," Current Opinion in Radiology **4**, 123–129 (1992).

[2]D. B. Kopans, "The positive predictive value of mammography," Am. J. Roentgenol. **158**, 521–526 (1991).

[3]M. Sabel and H. Aichinger, "Recent developments in breast imaging," Phys. Med. Biol. **41**, 315–368 (1996).

[4]F. Shtern, C. Stelling, B. Goldberg, and R. Hawkins, "Novel technologies in breast imaging: National Cancer Institute perspective," Society of Breast Imaging, Orlando, Florida, 153–156 (1995).

[5]L. V. Ackerman and E. E. Gose, "Breast lesion classification by computer and xeroradiograph," Cancer **30**, 1025–1035 (1972).

[6]J. Kilday, F. Palmieri, and M. D. Fox, "Classifying mammographic lesions using computerized image analysis," IEEE Trans. Med. Imaging **12**, 664–669 (1993).

[7]Z. Huo, M. L. Giger, C. J. Vyborny, U. Bick, P. Lu, D. E. Wolverton, and R. A. Schmidt, "Analysis of spiculation in the computerized classification of mammographic masses," Med. Phys. **22**, 1569–1579 (1995).

[8]B. Sahiner, H. P. Chan, N. Petrick, M. A. Helvie, D. D. Adler, and M. M. Goodsitt, "Classification of masses on mammograms using rubber-band straightening transform and feature analysis," Proc. SPIE **2710**, 44–50 (1996).

[9]B. Sahiner, H. P. Chan, N. Petrick, M. A. Helvie, and M. M. Goodsitt, "Computerized characterization of masses on mammograms: The rubber-band straightening transform and texture analysis," Med. Phys. **25**, 516–526 (1998).

[10]S. Pohlman, K. A. Powell, N. A. Obuchowshi, W. A. Chilote, and S. Grundfest-Broniatowski, "Quantitative classification of breast tumors in digitized mammograms," Med. Phys. **23**, 1337–1345 (1996).

[11]W. G. Wee, M. Moskowitz, N.-C. Chang, Y.-C. Ting, and S. Pemmeraju, "Evaluation of mammographic calcifications using a computer program," Radiology **116**, 717–720 (1975).

[12]S. H. Fox, U. M. Pujare, W. G. Wee, M. Moskowitz, and R. V. P. Hutter, "A computer analysis of mammographic microcalcifications: global approach.," Proceedings of the IEEE 5th International Conference on Pattern Recognition., IEEE, New York, 624–631 (1980).

[13]H. P. Chan, L. T. Niklason, D. M. Ikeda, and D. D. Adler, "Computer-aided diagnosis in mammography: Detection and characterization of microcalcifications," Med. Phys. **19**, 831 (1992).

[14]H. P. Chan, D. Wei, L. T. Niklason, M. A. Helvie, K. L. Lam, M. M. Goodsitt, and D. D. Adler, "Computer-aided classification of malignant/benign microcalcifications in mammography," Med. Phys. **21**, 875 (1994).

[15]H. P. Chan, D. Wei, K. L. Lam, S.-C. B. Lo, B. Sahiner, M. A. Helvie, and D. D. Adler, "Computerized detection and classification of microcalcifications on mammograms," Proc. SPIE **2434**, 612–620 (1995).

[16]H. P. Chan, B. Sahiner, K. L. Lam, D. Wei, M. A. Helvie, and D. D. Adler, "Classification of malignant and benign microcalcifications on mammograms using an artificial neural network," Proc. of World Congress on Neural Networks II, 889–892 (1995).

[17]H. P. Chan, D. Wei, K. L. Lam, B. Sahiner, M. A. Helvie, D. D. Adler, and M. M. Goodsitt, "Classification of malignant and benign microcalcifications by texture analysis," Med. Phys. **22**, 938 (1995).

[18]H. P. Chan, B. Sahiner, D. Wei, M. A. Helvie, D. D. Adler, and K. L. Lam, "Computer-aided diagnosis in mammography: Effect of feature classifier on characterization of microcalcifications," Radiology **197(P)**, 425 (1995).

[19]L. Shen, R. M. Rangayyan, and J. E. L. Desautels, "Application of shape analysis to mammographic calcifications," IEEE Trans. Med. Imaging **13**, 263–274 (1994).

[20]Y. Wu, M. T. Freedman, A. Hasegawa, R. A. Zuurbier, S. C. B. Lo, and S. K. Mun, "Classification of microcalcifications in radiographs of pathologic specimens for the diagnosis of breast cancer," Academic Radiology **2**, 199–204 (1995).

[21]Y. Jiang, R. M. Nishikawa, D. E. Wolverton, C. E. Metz, M. L. Giger, R. A. Schmidt, C. J. Vyborny, and K. Doi, "Malignant and benign clustered microcalcifications: automated feature analysis and classification," Radiology **198**, 671–678 (1996).

[22]D. L. Thiele, C. Kimme-Smith, T. D. Johnson, M. McCombs, and L. W. Bassett, "Using tissue texture surrounding calcification clusters to predict benign vs malignant outcomes," Med. Phys. **23**, 549–555 (1996).

[23]A. P. Dhawan, Y. Chitre, C. Kaiser-Bonasso, and M. Moskowitz, "Analysis of mammographic microcalcifications using gray-level image structure features," IEEE Trans. Med. Imaging **15**, 246–259 (1996).

[24]L. V. Ackerman, A. N. Mucciardi, E. E. Gose, and F. S. Alcorn, "Classification of benign and malignant breast tumors on the basis of 36 radiographic properties," Cancer **31**, 342 (1973).

[25]A. G. Gale, E. J. Roebuck, P. Riley, and B. S. Worthington, "Computer aids to mammographic diagnosis," Br. J. Radiol. **60**, 887–891 (1987).

[26]D. J. Getty, R. M. Pickett, C. J. D'Orsi, and J. A. Swets, "Enhanced interpretation of diagnostic images," Invest. Radiol. **23**, 240 (1988).

[27]C. J. D'Orsi, D. J. Getty, J. A. Swets, R. M. Pickett, S. E. Seltzer, and B. J. McNeil, "Reading and decision aids for improved accuracy and standardization of mammographic diagnosis," Radiology **184**, 619–622 (1992).

[28]Y. Wu, M. L. Giger, K. Doi, C. J. Vyborny, R. A. Schmidt, and C. E. Metz, "Artificial neural networks in mammography: Application to decision making in the diagnosis of breast cancer," Radiology **187**, 81–87 (1993).

[29]J. A. Baker, P. J. Kornguth, J. Y. Lo, M. E. Williford, and C. E. Floyd, "Breast cancer: Prediction with artificial neural network based on BI-RADS standardization lexicon," Radiology **196**, 817–822 (1995).

[30]J. Y. Lo, J. A. Baker, P. J. Kornguth, J. D. Iglehart, and C. E. Floyd, "Predicting breast cancer invasion with artificial neural networks on the basis of mammographic features," Radiology **203**, 159–163 (1997).

[31]H. P. Chan, B. Sahiner, N. Petrick, M. A. Helvie, K. L. Lam, D. D. Adler, and M. M. Goodsitt, "Computerized classification of malignant and benign microcalcifications on mammograms: texture analysis using an artificial neural network," Phys. Med. Biol. **42**, 549–567 (1997).

[32]J. H. Holland, *Adaptation in Natural and Artificial Systems* (University of Michigan Press, Ann Arbor, MI, 1975).

[33]D. E. Goldberg, *Genetic Algorithms in Search, Optimization, and Machine Learning* (Addison-Wesley, New York, 1989).

[34]B. Sahiner, H. P. Chan, N. Petrick, D. Wei, M. A. Helvie, D. D. Adler, and M. M. Goodsitt, "Image feature selection by a genetic algorithm: Application to classification of mass and normal breast tissue on mammograms," Med. Phys. **23**, 1671–1684 (1996).

[35]M. J. Norusis, *SPSS for Windows Release 6 Professional Statistics* (SPSS Inc., Chicago, IL, 1993).

[36]P. A. Lachenbruch, *Discriminant Analysis* (Hafner, New York, 1975), Chaps. 1, 3.

[37]C. E. Metz, J. H. Shen, and B. A. Herman, "New methods for estimating a binormal ROC curve from continuously-distributed test results," Annual Meeting of the American Statistical Association, Anaheim, CA (1990).

[38]H. P. Chan, S. C. B. Lo, B. Sahiner, K. L. Lam, and M. A. Helvie, "Computer-aided detection of mammographic microcalcifications: Pattern recognition with an artificial neural network," Med. Phys. **22**, 1555–1567 (1995).

[39]B. Sahiner, H. P. Chan, N. Petrick, D. Wei, M. A. Helvie, D. D. Adler, and M. M. Goodsitt, "Classification of mass and normal breast tissue: A convolution neural network classifier with spatial domain and texture images," IEEE Trans. Med. Imaging **15**, 598–610 (1996).

[40]R. M. Haralick, K. Shanmugam, and I. Dinstein, "Texture features for image classification," IEEE Trans. Syst. Man Cybern. **SMC-3**, 610–621 (1973).

[41]H. P. Chan, D. Wei, M. A. Helvie, B. Sahiner, D. D. Adler, M. M. Goodsitt, and N. Petrick, "Computer-aided classification of mammographic masses and normal tissue: Linear discriminant analysis in texture feature space," Phys. Med. Biol. **40**, 857–876 (1995).

[42]K. Fukunaga, *Introduction to Statistical Pattern Recognition*, 2nd ed. (Academic, New York, 1990), Chap. 3.

[43]H. P. Chan, B. Sahiner, R. F. Wagner, N. Petrick, and J. Mossoba, "Effects of sample size on classifier design: Quadratic and neural network classifiers," Proc. SPIE **3034**, 1102–1113 (1997).

[44]H. P. Chan, B. Sahiner, R. F. Wagner, and N. Petrick, "Classifier design for computer-aided diagnosis in mammography: Effects of finite sample size," Med. Phys. **24**, 1034–1035 (1997).

[45]R. F. Wagner, H. P. Chan, B. Sahiner, N. Petrick, and J. T. Mossoba, "Finite-sample effects and resampling plans: Applications to linear classifiers in computer-aided diagnosis," Proc. SPIE **3034**, 467–477 (1997).

[46]F. J. Ferri, P. Pudil, M. Hatef, and J. Kittler, "Comparative study of techniques for large-scale feature selection," Pattern Recognition in Practice IV, 403–413 (1994).

[47]W. Siedlecki and J. Sklansky, "A note on genetic algorithm for large-scale feature selection," Pattern Recogn. Lett. **10**, 335–347 (1989).

[48]C. E. Metz, P. L. Wang, and H. B. Kronman, "A new approach for testing the significance for differences between ROC curves measured from correlated data," in *Information Processing in Medical Imaging*, edited by F. Deconinck (The Hague, Martinus Nijhoff, 1984), pp. 432–445.

[49]B. Sahiner, H. P. Chan, N. Petrick, M. A. Helvie, D. D. Adler, and M. M. Goodsitt, "Classification of malignant and benign breast masses: Development of a high-sensitivity classifier using a genetic algorithm," Radiology **201**, 256–257 (1996).

[50]B. Sahiner, H. P. Chan, N. Petrick, M. A. Helvie, and M. M. Goodsitt, "Design of a high-sensitivity classifier based on genetic algorithm: Application to computer-aided diagnosis," Phys. Med. Biol. **43**, 2853–2871 (1998).

938 • 11:51 AM

Effects of Gadolinium (Gd-DTPA) Contrast Material on Single Voxel Proton Magnetic Resonance Spectroscopy

N.G. Campeau, MD, Rochester, MN • C.P. Wood, MD • B.J. Erickson, MD, PhD • C.R. Jack, Jr, MD • J.P. Felmlee, PhD

PURPOSE: To systematically study the effects of Gd-DTPA contrast material upon single voxel proton magnetic resonance spectroscopy (MRS) obtained on a 1.5 T clinical imager.

METHOD AND MATERIALS: A phantom containing physiologic concentrations of the major brain metabolites (NAA, Cr, Cho, mI) was constructed. Using the standard birdcage headcoil, multiple 3.0 cm^3 single voxel STEAM and PRESS spectra were acquired from the center of the phantom using the PROBE software package (General Electric, Milwaukee WI). For each acquisition type, all parameters were kept constant except Gd-DTPA concentration which ranged from 0.0 to 2.0 mmol/litre. The area of the NAA, Cr, Cho and mI peaks, as well as the NAA/Cr, Cho/Cr, and mI/Cr peak ratios were obtained using the PROBE/SV QUANT analysis package. The signal to noise ratio (SNR) and rms noise of the Cr peak were also determined for all acquisitions.

RESULTS: With both STEAM and PRESS localization, spectra acquired with increased Gd-DTPA demonstrated spectral broadening and marked alteration of both the peak heights and areas. These changes were first manifested in the higher (>2.5) ppm range of the spectrum. The Cho peak loses signal rapidly with increasing Gd-DTPA concentration, falling to approximately 50% of its initial value at 1.0 mmol/litre. NAA is the least affected by Gd-DTPA. Cr and mI signal fall off at a slightly decreased rate compared to Cho. The SNR of the Cr peak decreases to less than 20% of the precontrast value at 2.0 mmol/liter Gd-DTPA concentration. Similarly there was a 300-700% increase in rms noise of the Cr peak.

CONCLUSIONS: The effects of Gd-DTPA on proton MRS were systematically demonstrated for single voxel STEAM and PRESS acquisitions. MRS performed following administration of Gd-DTPA produces demonstrable chnages in both peak areas and ratios of the major brain metabolites. These results are important clinically, and suggest that MRS is best performed prior to Gd-DTPA administration.

Wednesday Morning • Room S404AB

■ Physics (Computer-aided Diagnosis: Mammography)

In joint sponsorship with the American Association of Physicists in Medicine

PRESIDING: **Heang-Ping Chan, PhD**, Ann Arbor, MI

Computer Code: M04 • 1½ hours

To receive credit, relinquish attendance voucher at end of session.

939 • 10:30 AM

Computerized Classification of Mammographic Masses Using Morphological Features

B. Sahiner, PhD, Ann Arbor, MI • H. Chan, PhD • M.A. Helvie, MD • T.E. Wilson, MD • S. Sanjay-Gopal, PhD • N.A. Petrick, PhD

PURPOSE: Both morphological and texture features are potentially useful for computerized characterization of breast masses on mammograms. A characterization method based on texture features was previously developed in our laboratory. Our purposes in this study were (i) to evaluate the effectiveness of morphological features for computerized classification of malignant and benign breast masses, and (ii) to improve classification accuracy by combining texture and morphological features.

METHOD AND MATERIALS: Our data set included 205 biopsy-proven masses, of which 100 were malignant and 105 were benign. Four of the benign masses and 47 of the malignant masses were spiculated. Texture features were extracted from images processed with the previously-developed rubber-band straightening transform. For morphological feature extraction, boundaries of the masses were manually delineated by two MQSA-approved radiologists. The morphological features evaluated in this study included Fourier descriptors, convexity measures, normalized radial length statistics, contrast, circularity, area, perimeter, and the perimeter-to-area ratio.

RESULTS: The best two morphological features were the Fourier descriptor summary feature (A_z =0.87) and the convex hull area measure (A_z =0.84). When the Fourier descriptor summary feature and four texture features were combined in a linear discriminant classifier, the area under the ROC curve was 0.91 using leave-one-case-out test scores. In comparison, for the classification of the same set of masses, the accuracy of the two radiologists were A_z =0.91 and 0.88.

CONCLUSIONS: The morphological features extracted from the mass shapes were effective for classification of the masses as malignant or benign. The use of texture features in addition to morphological features in a linear classifier improved the classification accuracy. We are currently evaluating morphological features extracted from automatically segmented mass shapes.

940 • 10:39 AM

Computer-aided Diagnosis in Screening Mammography: Detection of Missed Cancers

R.M. Nishikawa, PhD, Chicago, IL • M.L. Giger, PhD • R.A. Schmidt, MD • D.E. Wolverton, MD • S.A. Collins, BS • K. Doi, PhD • et al

PURPOSE: To analyze the performance of our CAD detection schemes used prospectively on screening mammograms.

METHOD AND MATERIALS: We have analyzed over 14,500 screening cases using our automated detection schemes for masses and clustered microcalcifications. We have performed follow-up analyses on the first 10,000 cases.

RESULTS: Sixty-seven women in our study cohort developed breast cancer. The computer was able to detect approximately 65% of these cancers at a false-positive rate of 2.0 false masses and 0.9 false clusters per image. More importantly, there were 20 cancers in which the patient had a previous negative mammogram included in our study. Three of the 20 were mammographically negative, even in retrospect. In the remaining 17 cases, the computer was able to detect the cancer in 8 of them. Three of the 8 were interpretation misses by the radiologist, while the other 5 were observational misses.

CONCLUSIONS: In a non-prevalence screening population, our computer-aided detection schemes are capable of detecting up to 25% (5/20) of screening-detected cancers a year or more before detected by the radiologist.

This work was supported in part by grants from the NIH (CA 60187 and T32 CA09649), US Army (DAMD17-96-1-6058 and DAMD17-96-1-6228) and R2 Technology, Inc. RMN, MLG, RAS, and KD are shareholders in R2 Technology, Inc., Los Altos, CA **[See also *info*RAD exhibit 9103.]**

941 • 10:48 AM

Computer-aided Diagnosis in Ultrasound: Classification of Breast Lesions

M.L. Giger, PhD, Chicago, IL • C.J. Moran • D.E. Wolverton, MD • H.A. Al-Hallaq, MSc • Z. Huo, PhD

PURPOSE: To develop methods for the computer analysis of lesions in ultrasound images of the breast.

METHOD AND MATERIALS: A database of ultrasound images were collected from 39 patients. Benign lesions were confirmed by biopsy, cyst aspiration, or followup while malignant lesions were confirmed by biopsy. Regions of interest within the ultrasound scan of the breast lesion and deep to the lesion were extracted for computer analysis. Various features were then extracted including those related to lesion margin, texture within the lesion, lesion shape, and the nature of the posterior acoustic attenuation pattern. ROC analysis was used to evaluate the performance of the various features in distinguishing benign from malignant lesions.

RESULTS: ROC analysis of the computer-extracted features yielded Az values of 0.82, 0.88, and 0.84 for features based on the texture, margin, and posterior acoustic attenuation, respectively, in the task of distinguishing between benign and malignant lesion images. Az values up to 0.82 were obtained in the task of distinguishing images of malignant from images of benign lesions that were proven by either cyst aspiration or biopsy.

CONCLUSIONS: Our results indicate that the computerized analysis of ultrasound images has the potential to increase the specificity of breast sonography.

M. L. Giger is a shareholder in R2 Technology, Inc. (Los Altos, CA). **[See also scientific exhibit 0071BR.]**

942 • 10:57 AM

Comparison of Local Clustering and Gradient-based Region Growing Segmentation for the Automated Detection of Masses on Digitized Mammograms

N.A. Petrick, PhD, Ann Arbor, MI • H. Chan, PhD • B. Sahiner, PhD • M.A. Helvie, MD • L.M. Hadjiiski, PhD • M.M. Goodsitt, PhD

PURPOSE: We have developed a local clustering technique for the segmentation of breast structures in an automated mass detection algorithm. In this study, we compared the accuracy of this new technique with a previously developed gradient-based region growing technique.

METHOD AND MATERIALS: We have developed two different segmentation techniques for improving the border definition of breast structures initially identified with a density-weighted contrast enhancement (DWCE)

Wednesday

algorithm. The first technique used gradient-based region growing applied to the DWCE objects. The second technique used local clustering based on feature images derived from background-corrected ROIs defined by the DWCE objects. The feature images consisted of a median filtered and two edge-enhanced versions of the ROI along with the original region. Using this information, the ROI pixels were clustered into either the object representing the detected breast structure or its surrounding background. Morphological and then texture based false-positive (FP) reduction followed the segmentation. The effect of the two techniques on the overall accuracy of breast mass detection was evaluated using free-response receiver operating characteristic (FROC) analysis.
RESULTS: For a data set of 253 mammograms each containing a biopsy-proven mass, both methods had an initial sensitivity of over 97%. Morphological FP reduction following clustering in comparison with morphological FP reduction after region growing reduced the number of detected objects from 37 to 29 per image. The final FROC performance after texture classification was also improved with the clustering technique. At a sensitivity of 80%, clustering reduced the number of FPs/image to 1.3 as compared to 1.9 FPs/image with region growing (*i.e.*, a 32% reduction).
CONCLUSIONS: Local clustering improves object segmentation and reduces FP detections in our automated detection scheme.

943 • 11:06 AM

Computerized Analysis of Parenchymal Patterns for the Assessment of Breast Cancer Risk

Z. Huo, PhD, Chicago, IL • M.L. Giger, PhD • O.I. Olopade, MD • S.A. Cummings, MSc

PURPOSE: To develop computerized methods that relate mammographic features to breast cancer risk and to study the feasibility of using such features along with age to identify women at risk.
METHOD AND MATERIALS: 392 cases were collected into two categories: low-risk group and high-risk group including some BRCA1/BRCA2 mutation carriers. Regions-of-interest (ROIs), 256 pixels by 256 pixels in size, were selected from the central breast region within digitized mammograms. Various computer-extracted features were then calculated to evaluate the variation of texture within an individual's mammogram. Also, the lifetime risk and 10-year risk were calculated for each case using the clinical models proposed by Gail et al., and by Claus et al. The ability of each computer-extracted feature was evaluated using ROC analysis in the task of distinguishing between low-risk cases and gene-mutation carriers (using all cases and an age-matched subgroup). In addition, correlation analysis was performed between the computer-extracted features and the calculated clinical markers of risk from the Gail and Claus models.
RESULTS: Both linear discriminant analysis and artificial neural networks achieved an area under the ROC curve of 0.91 in distinguishing between low-risk cases and gene-mutation carriers. Linear regression analysis of the computer-extracted features along with age yielded $r=0.62$ ($p<0.0001$), similar to the correlation of 0.61 calculated between the Gail model and the Claus model.
CONCLUSIONS: Computerized analysis of mammographic parenchymal patterns can provide an objective characterization of mammographic parenchymal patterns that may be associated with breast cancer risk.
M. L. Giger is a shareholder in R2 Technologies, Inc. (Los Altos, CA).

944 • 11:15 AM

Applying Genetic Algorithms for the Selection of Features for Computer-assisted Diagnosis in Mammography

B. Zheng, PhD, Pittsburgh, PA • Y. Chang, MS • W.F. Good, PhD • X. Wang, MD, PhD

PURPOSE: Feature selection has a large impact on the performance of computer-assisted diagnosis schemes (CAD) for mammography. By using a genetic algorithm (GA) to optimize the feature set for CAD, this study investigated a promising approach for improving CAD performance and robustness.
METHOD AND MATERIALS: 1,557 images were processed by our CAD scheme, after which 742 positive mass regions and 6,040 suspicious negative regions were selected. These regions were randomly divided into one training and two testing datasets. In each region, 32 features were extracted. Two different classifiers, an artificial neural network (ANN) and a Bayesian belief network (BBN), were trained to identify positive and negative regions based on a subset of features selected by the GA. The maximum area under ROC curve (Az) was used as GA fitness criterion. For each iteration of the GA a subset of features was selected, after which both the ANN and BBN were trained with the training set, and then the first testing set was used to evaluate fitness. Finally, after GA optimization, performance and robustness of two networks were evaluated and compared on the second testing set.
RESULTS: Using GA optimization, more than half of initial 32 features were eliminated from the active nodes of two networks. Although different features were selected in the two networks, there was no difference in their final performance. Both yielded Az = 0.86 for the second testing set. The Az values for the optimized subsets of features were significantly higher than those attained by using all 32 features (i.e., 0.81 and 0.79 for the ANN and BBN, respectively).
CONCLUSIONS: A GA using an appropriate fitness criterion can provide an effective approach to feature selection, and hence, to the optimization of CAD performance and robustness. Since the two classifiers considered here, which were based on totally different machine learning and inference mechanisms, converged to the same performance level, this study also suggests that ultimately the limits on performance may be more dependent on feature set than on any particular inference paradigm.

945 • 11:24 AM

Characterization of Malignant and Benign Masses on Mammograms Based on a Hierarchical Classifier

L.M. Hadjiiski, PhD, Ann Arbor, MI • B. Sahiner, PhD • H. Chan, PhD • N.A. Petrick, PhD • M.A. Helvie, MD • M.M. Goodsitt, PhD

PURPOSE: To evaluate the accuracy of a hierarchical classifier for classification of malignant and benign masses.
METHOD AND MATERIALS: A hierarchical classifier which combines an unsupervized adaptive resonance network (ART2) and a supervised linear discriminant classifier (LDA) was developed for analysis of mammographic masses. At the first stage, the ART2 network separated the masses into different classes based on the similarity of the input feature vectors. At the second stage, a separate LDA model was formulated within each class to classify the masses as malignant or benign. In order to examine the utility of this approach, a database of 253 regions of interest containing biopsy-proven masses was used. A texture feature set was extracted and stepwise feature selection was used to find a subset of features for discrimination of spiculated and non-spiculated masses. The ART2 network classified the data set into three classes based on these features. One of the classes contained predominantly spiculated masses which corresponded to a higher fraction of malignant masses. For each class, stepwise feature selection was again used to determine the optimal feature subset for classification of malignant and benign masses using LDA. The classification accuracy of the hierarchical classifier was analyzed by receiver operating characteristic (ROC) methodology with a leave-one-case-out training and testing resampling scheme.
RESULTS: The areas, A_z, under the ROC curve for the three classes were found to be 0.94, 0.86 and 0.95. In addition, approximately 48% of the benign masses could be identified without missing a malignant mass, compared to 41% with LDA classification alone.
CONCLUSIONS: The ART2 network is useful for unsupervised clustering of cases into classes based on the similarity of their properties. This facilitates further classification of the cases within each class.

946 • 11:33 AM

The Effect of Computer-aided Diagnosis on Diagnostic Performance

M. Ikeda, MD, PhD, Nagoya City, Japan • T. Ishigaki, MD, PhD • K. Yamauchi, MD, PhD

PURPOSE: To evaluate the effects of CAD outputs as a "second opinion" on radiologists' performance in detection diagnosis by image-reading study.
METHOD AND MATERIALS: We have studied the effects of 25 kinds of simulated CADs with various sensitivities and specificities (from 60% to 100%) on diagnostic performance. Six novice radiologists read 100 signal pulse noise images and 100 noise-only images that were produced by computer and randomly displayed on CRT. They reported their probability judgments regarding the presence of a line in the background Gaussian white noise. The radiologists' performance was evaluated with receiver operating characteristic (ROC) analysis, and A_z (the area under the binormal ROC curve) was used as an index of performance. The difference among A_z's of 25 kinds of image-reading experiments was analyzed by the analysis of variance (ANOVA) of pseudovalues computed by the jackknife method proposed by Dorfman et al.
RESULTS: Three-way non-repeated ANOVA revealed significant differences in the diagnostic performance among 25 kinds of CAD ($p < 0.001$), and showed a significant effect of some kinds of CAD on an increase in the radiologists' performance ($p < 0.05$). The overall accuracy of CAD outputs were positively correlated with the radiologists' performance ($r=0.933$), and the correlation between the sensitivity of CAD outputs and the radiologists' performance ($r=0.706$) was better than between the specificity of CAD and the performance ($r=0.614$).
CONCLUSIONS: 1) The diagnostic performance with the aid of CAD systems with rather good accuracy is better than without it. 2) The overall accuracy of CAD outputs is the most effective factor affecting radiologists' performance in detection diagnosis. Here, in cases in which the overall accuracy of CAD outputs is the same, radiologists' performance would be